Site formation processes of outdoor spaces in tropical environments: a micro-geoarchaeological case study from backyard Lo Gach, southern Vietnam

Elle Grono[a,b*], David E. Friesem[b,c], Rachel Wood[a], Tim Denham[a], Nguyen Khanh Trung Kien[d], Dang Ngoc Kinh[d], Philip J. Piper[a]

[a] School of Archaeology and Anthropology, Australian National University, Canberra, ACT 2601, Australia
[b] Department of Maritime Civilizations, School of Archaeology and Maritime Cultures, University of Haifa, Mount Carmel, Haifa, 3498838, Israel
[c] Haifa Center for Mediterranean History, University of Haifa, Haifa, Israel
[d] Centre for Archaeology, Southern Institute of Social Sciences, Ho Chi Minh City, Vietnam

ABSTRACT:

In the tropics, outdoor areas are important arenas of social life and the scene of economic and daily activities. Yet, outdoor areas are not often detected due to destructive post-depositional processes and low archaeological visibility. Here we use microarchaeology to establish the settlement history and outdoor use of space at Lo Gach in Long An Province, southern Vietnam. The radiocarbon chronology identifies two phases of occupation: an initial presence at 3300-3000 cal. BP; and, later activity at 2750-2400 cal. BP. Microarchaeological analysis of the stratigraphy reveal complex sequences of organic waste severely transformed by chemical diagenesis. The results indicate that the excavated area at Lo Gach was an outdoor 'backyard' containing external surfaces utilised for a range of activities including rice processing, disposal of combustion residues, in situ *burning, and recurrent foot traffic. Intensified rice agriculture and the systematic management of organic waste were the main structuring rhythms of social life that were performed at the Lo Gach settlement.*

KEYWORDS

Southeast Asia, metal age, agricultural transition, microarchaeology, use of space, waste management

1. INTRODUCTION

Outdoor areas are often underrepresented in archaeological contexts, especially in the tropics, and this underrepresentation is a source of significant bias in the study of past activity areas. In hot, humid tropical regions, outdoor spaces such as open-air patios, yards and gardens are important arenas for social life, commonly utilised as intensive activity areas beyond the confines of habitation structures (Bernot 1982; Waterson 1990; Robin 2002; Robin and Rothschild 2002; Hutson et al. 2007; Friesem and Lavi 2017). Outdoor activity residues left behind following site maintenance and cleaning practices comprise perishable organic remains that are prone to poor preservation, exacerbated by the warm and humid conditions of the tropics (Friesem et al. 2016; Friesem and Lavi 2017; Morley and Goldberg 2017; Sulas et al. 2017). Burial environments exposed to the weather are significantly more reworked by post-depositional processes relative to indoor spaces (Matthews and Postgate 1994; Matthews 2005; Shillito and Ryan 2013; Banerjea et al. 2015b). The combination of cultural and natural site formation processes therefore results in low archaeological preservation and visibility of outdoor activity areas, and thus biases our understanding of the use of space within settlements. The difficulties involved in the detection of outdoor spaces in the tropics may be an important factor contributing to the absence of settlement evidence in Mainland Southeast Asian (MSEA) prehistory (Grono 2020). Very few prehistoric settlements have been detected (Henriksen 1982; Nitta 1991; O'Reilly 1997; Nishimura and Nguyen 2002; Higham et al. 2014; Piper and Oxenham 2014; Oxenham et al. 2015; Higham 2017; Piper et al. 2017) and the social and economic structuring of internal and external spaces is largely unexplored.

---

* corresponding author: egrono@campus.haifa.ac.il
https://orcid.org/0000-0002-3607-6686

Here, we report on the use of outdoor spaces at Lo Gach, a prehistoric settlement in southern Vietnam that was excavated in 2014. Our investigations were designed to reconstruct site formation processes and had three main aims: (1) identify use of space; (2) characterise post-depositional processes; and, (3) place these within a temporal framework. To meet the first two aims, we employ a microarchaeological approach integrating micromorphology with Fourier Transform Infrared (FTIR) spectroscopy and phytolith concentrations. Microarchaeology is routinely used to understand site formation processes at archaeological settlements in Southwest Asia and Europe, however it has been vastly underutilised in the tropics (Stephens et al. 2005, 2017; Lewis 2007; Simpson et al. 2008; Kourampas et al. 2009; Sulas and Madella 2012; Friesem et al. 2016; Morley and Goldberg 2017; Morley et al., 2017; Sulas et al. 2017; Villagran et al. 2017b; McAdams et al. 2020). Regionally in MSEA, very few open-air sites have been investigated using microarchaeology (Grave and Kealhofer 1999; Grono 2020). To investigate aim 3, a Bayesian model was built incorporating radiocarbon and stratigraphic information. Our research establishes the nature and chronology of human practices at Lo Gach which appear to have been performed outdoors and to have centred around agricultural processing and the management of organic waste at the settlement.

2. LO GACH SITE

Lo Gach (10°54’58”N/105°43’50”E) is located approximately 1-2 m above sea level on the west bank of the Vam Co Tay River in Vinh Tri commune, Vinh Hung district, Long An Province, southern Vietnam (Fig. 1). The site is located in the humid tropics and has a monsoonal climate with distinct wet and dry seasons. The region has an average temperature of 27-30°C that is relatively uniform throughout the year (Nguyen et al. 2000: 427) and an average annual precipitation of 1000–2000 mm that falls mainly in the wet season between April and October (Hori 2000).

Lo Gach was first discovered in 1989 and preliminary excavations of 4m^2 were undertaken by Long An Provincial Museum in 2003. In 2005, the Institute of Archaeology (Hanoi) excavated a further 24m^2. The investigators identified a complex sequence of cultural layers between 0.9-1.2 m deep, consisting of ‘grey earth mixed with fine sand’ containing high concentrations of pottery, animal bone and osseous artifacts (Bui 2008). No chronometric dating was undertaken, but based on comparisons between the material culture from Lo Gach, and other key metal age[1] sites in southern Vietnam such as Go O’Chua (another settlement to the northwest on the Vam Co Tay River), Con Son, Go Dinh and Rach Rung it was estimated that the settlement was occupied between c. 2500-2200 years ago (Bui 2008: 44). In 2012, the Centre for Archaeology, Southern Institute of Social Sciences (Ho Chi Minh City) in collaboration with Long An Provincial Museum undertook another test excavation (2012 Trial Trench) in the middle of the Lo Gach settlement site. They identified a very well-preserved archaeological sequence of floor surfaces and midden deposits up to 1.5 m in depth. Four radiocarbon dates from the top to bottom of the stratigraphy indicated occupation likely took place between 2700-2500 cal. BP, some 200-300 years earlier than had been estimated using typological sequencing.

The results of the excavations in 2005 and 2012 provided the foundations of enquiry for the 2014 investigations, a collaboration between the Centre for Archaeology, Southern Institute of Social Sciences (Ho Chi Minh City), Long An Provincial Museum and the Australian National University. Three trenches were excavated during the 2014 season. Trench 1 (5 m x 4 m) was located adjacent

---

[1] Terminology for MSEA chronological periodisations including neolithic, bronze age and metal age periods are rendered in the lower case to disassociate the terms from inherent cultural evolutionary associations, and to distance MSEA prehistoric sequence from chronological frameworks developed in Europe and the Near East that are inappropriate to the Southeast Asian region.

to the 2012 Trial Trench and Trench 2 (3 m x 2 m) in close proximity to the 2006 excavation trench. Trench 3 (3m x 2m) was excavated close to the current river, and was primarily undertaken to observe the spatial distribution of archaeological deposits and the effects of river bank erosion on the preservation of the archaeological site (Fig. 2). With the exception of radiocarbon dating in Trench 3, this manuscript will focus on Trenches 1 and 2 (Table 1) from the 2014 excavation. When describing the 2014 excavation results below, context (C. numbers) refer to contiguous deposits that extended over all or most of an excavation trench whereas feature (F- numbers) reference either discontinuous (patchy) deposits or pits and postholes.

2.1. TRENCH 1 (2014 EXCAVATION):

The stratigraphy was dominated by organic materials, silicified plant remains, charcoal and burnt sediments that were distributed in thin stratigraphic layers that sloped markedly from the slightly raised ground furthest from the river in the east, to the west (Fig. 2c). Beginning at a depth of c. 10 cm below the modern ground level, a series of compacted activity surfaces were recorded [e.g., bottom to top in the west wall sequence shown in Fig. 2c: F1-141, F1-127, F1-126, F1-123, F1-125, F1-122, F1-119, F1-113, F1-110, F1-109, F1-108, F1-107, F1-62] (Table 1, Fig. 2c). These deposits typically consisted of two distinguishable layers: an upper hard compacted light creamy-grey surface composed of friable loamy sands, underlain by a layer of soft dark greyish brown to black organic and humic sediments rich in charcoal and ash. Pottery, burnt clay, silicified rice remains, and leaf and woven matting impressions were occasionally visible in and/or on the surfaces (Fig. S1.1; Cameron 2017). Several thin layers (3 cm thick) of silicified plant remains (predominantly rice chaff) could be identified on the surface of several of these deposits, especially in the east and central areas of the Trench [F1-119, F1-122, F1-126] (Table 1, Fig. 2c).

Below the compacted feature deposits was a homogenous, relatively pure layer [C.103] of pale creamy-grey silt laterally continuous across most of the trench and devoid of archaeological materials. This was interpreted in the field as a deliberately laid foundation surface of fine sediment. Below C.103, initial human activities in Trench 1 are represented by loamy sand [C.104] and sandy surfaces [F1-127, F1-140, F1-157]. These overlay a mixed, reworked deposit of natural sand and gravel [C.105] containing high concentrations of reworked pottery, animal bones and evidence of bronze working (bronze arrowhead and casting molds). Basal deposits are natural sterile alluvial sediments [C.106].

Several small postholes were identified throughout the archaeological sequence, indicating the construction of lightweight wooden structures. There was no evidence for the construction of more substantial dwellings. Many of the hard compacted activity surfaces were only evident at the west end of the trench, terminating towards the middle. This suggests that Trench 1 was located towards the periphery of the area of everyday human activity, and that habitation (namely, any structures) was located towards the east, away from the bank of the river. The observed stratigraphic sequence within Trench 1 demonstrated that the deposition of deposits had slowly migrated westwards towards the contemporary river. The stratigraphic interpretation is supported by chronometric dating that shows most deposits at the east end of Trench 1 are older than those to the west, as well as older than the archaeological sequence recorded in Trench 3.

2.2. TRENCH 2 (2014 EXCAVATION):

The upper horizons of Trench 2 were similar to deposits encountered in Trench 1, including hard, compacted surfaces [F2-7, F2-42, F2-53] and loose dark grey sandy loam deposits [C.202, C.203] containing high quantities of burnt organic materials and ash (Table 1, Fig. 2a). These overlay a sequence of dark brown sandy loams [C.204 and C.205] containing high concentrations of charcoal, pottery and animal bone. No evidence of bronze working was identified in the lower layers of Trench 2, which were the only layers recorded in the 2014 excavations dated to before 3000 cal. BP (see dating below). However, one part of a double-sided stone casting mold was recovered from the adjacent 2005 trench, in 'Layer 8', close to the base of the excavations.

These deposits recorded during previous excavations potentially correspond to deposits near the bottom of Trench 2. This would suggest that metallurgy possibly arrived in the Mekong region of southern Vietnam sometime before 3000 cal. BP (Bui 2008: 44). The 2012 and 2014 excavations demonstrated that bronze metallurgy was certainly present by 2750 cal. BP. An overview of all the material culture recovered from the 2014 excavations is provided in Supplementary Information 1.

3. MATERIALS AND METHODS

3.1. Radiocarbon Dating

Thirty-two radiocarbon dates on 29 single entity samples (charcoal (n=27) and rice grain (n=2)) were obtained from the Trial Trench (n=5), and Trenches 1 (n=13), 2 (n=7) and 3 (n=7) (Supplementary Information 2) and calibrated in OxCal v.4.4 (Bronk Ramsey 2009a) against a 50:50 mixture of IntCal20 (Reimer et al. 2020) and SHCal20 (Hogg et al. 2020) as Vietnam falls within the Intertropical Convergence Zone where the two hemispheres mix. Two Bayesian models were run in OxCal as the majority of samples were charcoal which may be older than their contexts due to the ‘old wood effect’. The first (A) used the General t-type Outlier Model for all sample types, assuming that most dates are accurate, although some may be older or younger than their context (Bronk Ramsey 2009b). The second (B) used the Charcoal Plus Outlier Model to explore the impact of the ‘old wood effect’. This Model allows most dates on charcoal to be older than their context, with just a small probability that dates may be too young. Despite some minor differences in the age estimate for the end of the sequence, we favour model B as it is likely to reflect the impact of the inbuilt age of charcoal more appropriately, and agrees more closely with the stratigraphic relationships observed between the trenches. Therefore, we only discuss the results of model B here but present both models in Supplementary Information 2. All distributions are given at 95% probability.

3.2. Microarchaeology

The microarchaeological protocol used a tripartite methodology consisting of: contextual sedimentary analysis using micromorphology; mineralogical analysis achieved through Fourier Transform Infrared (FTIR) spectroscopy; and, characterisation of plant remains by phytolith concentrations (following similar methodological approaches by Shahack-Gross et al. 2004; Shahack-Gross et al. 2005; Friesem et al. 2014; Regev et al. 2015).

Micromorphology is contextual sedimentary analysis conducted on thin sections prepared from undisturbed stratigraphic blocks that preserve the contextual arrangement of a deposit, enabling inferences on composition and formation history (Courty et al. 1989; Macphail and Goldberg 2017; Nicosia and Stoops 2017; Karkanas and Goldberg 2018). During excavations six intact blocks of feature deposits were removed, and following completion of excavations 13 kubiena tins of undisturbed stratigraphy were extracted from the east and west walls of Trench 1 and six kubiena tins were removed from the west wall of Trench 2 for microarchaeological analyses (Fig. 2). Microstratigraphic unit (MSU) numbers allocated during micromorphological analysis define multiple microlayers within thin sections. Refer to Supplementary Information 3 for thin section preparation and analysis protocols.

FTIR and phytolith concentrations are compositional sedimentary analyses. FTIR provides identification of organic and mineral components and information on the alteration state of minerals resulting from heating or diagenesis (Weiner 2010). A rapid phytolith extraction and concentration method (Katz et al. 2010) is used to obtain a comparative measure of the relative concentrations of phytoliths and diatoms between deposits. The method provides a relative indicator of cultural inputs of silica bodies into the sediments (e.g., cultural use of phytolith-bearing plants including rice, or use of local diatom-rich clays to prepare floor plasters) as well as natural inputs from background vegetation and pedogenesis. FTIR and phytolith analyses were conducted on sediments extracted from the 'mirror image' faces of the micromorphological thin sections of kubiena tins and intact deposits, producing results that correlate closely to microstratigraphic units within the thin sections. Microarchaeological analytical protocols are described in detail in Supplementary Information 3.

Microarchaeological results are synthesised and described using microfacies analysis. Microfacies (mF) analysis is an approach which groups together deposits with similar microarchaeological (e.g., micromorphology, FTIR spectral composition, phytolith concentrations) attributes that reflect a shared formation history or depositional process (Courty 2001). Within archaeological sites, the concept of microfacies acknowledges the influence of repeated human activities on site formation, affording insights into habitual practices and routines (e.g., Goldberg et al. 2009; Villagran et al. 2011; Karkanas and Van De Moortel 2014).

4. RESULTS

4.1. RADIOCARBON DATING

The calibrated unmodelled and modelled radiocarbon dates using the Charcoal Plus Outlier Model (Model B) models are shown in Table 2 and Fig. 3 (see Fig. S2.1 in Supplementary Information 2 for Model A). The two models mostly demonstrate good agreement between stratigraphic context, trench and chronological age. The oldest deposits are found at the base of Trench 2, starting at 3290-2942 cal. BP (Table 3). A possible hiatus between around 2800 and 3000 cal BP is observed between contexts F2-42 (Phase I) and F2-13 (Phase II), with calibrated unmodelled dates of 3074-2788 cal. BP (S-ANU38837) (F2-42) and 2758-2547 cal. BP (S-ANU38836) (F2-13) (Table 2, Fig. 3, Fig. S2.1). The Trench 2 Phase II sequences are similar to those in Trench 1, where deposition commenced at 2737-2527 cal. BP (Table 3). This corresponds closely to similar deposits in the adjacent Trial Trench, which start at 2716-2528 cal. BP (Model B). Model B predicts that occupation of Trench 2 ends at 2721-2402 cal. BP, the Trial Trench at 2621-2448 cal. BP, and Trench 1 at 2622-2492 cal. BP (Table 3). The Phase I and II archaeological sequence in Trench 2 suggests complete site occupation lasted between 277-787 years starting around c. 3300-3000 cal. BP. The later phase of occupation at Lo Gach (Phase II) is most precisely recorded in Trench 1, and this indicates the deposits have accumulated rapidly, and site occupation lasted less than 220 years, sometime between ~2750 and 2400 cal. BP.

4.2. MICROFACIES TYPES AND THEIR USE OF SPACE CORRELATES

Microarchaeological analysis of 29 archaeological thin sections from Lo Gach identified 77 microstratigraphic units (MSUs) representing five microfacies (mFs). Microarchaeological results are reported according to mF types, denoted by alphabetical letters, that reflect different formation histories and specific uses of space. The mF types are described in terms of primary observations and derivative interpretations. Microarchaeological attributes of the mF types are summarised in Table 4. Supplementary Information 4 provides full micromorphological descriptions (Table S4.1), FTIR spectral graphs (Fig. S4.1) and phytolith concentration values (Table S4.3).

4.2.1. MICROFACIES A AND B: MIDDEN DEPOSITION OF BURNT COMPONENTS

Microfacies A and B are comprised predominantly of by-products of combustion activities: In mF A, ashes are dominant (Fig. 4a-4d); in mF B carbonised plant residues predominate (Fig. 4e-4g). The degree to which plant residues are pyrogenically altered to form ashed or charred remains is dependent on temperature, oxygen availability and composition (Braadbaart and Poole 2008). Ashes form in oxidised combustion environments (Braadbaart and Poole 2008: 2435) and in high temperature fires exceeding 500°C for woody plants rich in calcium oxalate crystals that produce calcitic ashes and 800°C for phytolith-rich plants (e.g., grasses or reeds) that produce vitrified (melted) siliceous slags (Brochier and Thinon 2003; Canti 2003; Canti and Brochier 2017). Two subvariants of mF A are distinguished. Microfacies A^1 comprises microcrystalline (crystallitic XPL) calcitic plant ashes (Fig. 4a, Fig. 4c, Table 4) and has an FTIR mineralogical composition of calcite, aragonite (likely pyrogenically-formed in the presence of burnt residues; see Toffolo and Boaretto 2014) and altered (heated) clay (Fig. 5c, Table 4). Microfacies A^2 comprises a vesicular and spongey grey (PPL) white (OIL) isotropic (XPL) fabric of vitrified (melted) phytoliths and has an FTIR composition of opal (phytoliths) and glass (melted phytolith slags) (Fig. 4b, Table 4). This subdivision allows correlation of particular episodes of midden deposition with specific fuel types: woody plants in mF A^1 and grasses in mF A^2 (Canti 2003; Braadbaart et al. 2012). A third subvariant, mF A^3, relates to post-depositional biological transformation of the ash deposits by soil fauna (Table 4).

The ashes became saturated following deposition, leading to compaction of the deposits, loss of microstructure, and chemical alteration. Ashes variably underwent: recrystallisation, resulting in indurated masses of calcium carbonate (Fig. 4a, Fig. 4c; Karkanas et al. 2007); phosphatisation, resulting in cryptocrystalline orange (PPL) isotropic (XPL) groundmasses (Fig. 4d) and indicated by the presence of carbonated hydroxyapatite (CHAP) identified in FTIR spectra (Table 4) (Goldberg et al. 2009; Villagran et al. 2017b); and, decalcification, resulting in mosaic and isotropic (XPL) fabrics heavily stained with iron and manganese oxides (Table 4). Diatom concentrations (<3,335 diatoms/g sed[2]) may indicate autochthonous formation in a wet burial environment during saturated conditions at the site (see Grono et al. 2022). This suite of post-depositional processes indicates fluctuating wetting and drying conditions, suggesting that the deposits were located in an outdoor area exposed to the weather.

Charcoal, the dominant component in mF B, forms in low temperature fires (between 350°C and 500°C) and oxygen-reduced parts of fires (Braadbaart and Poole 2008). Carbonised plant residues in mF B include: dicotyledon wood species, identified based on observation of concentric and circular patterning of xylem vessels of hardwoods; softwoods, identified based on rectilinear cell structures (Canti 2017); and monocotyledon species, including rice husks (Fig. 4e). FTIR analyses identify the presence of altered clay, charcoal, gypsum, opal (phytoliths), quartz and CHAP (Table 4). Two subvariants of mf B distinguish between concentrations of small carbonised plant fragments in a matrix of phosphatised ashes [mF B^1] (Fig. 4e-4g) and large, horizontally-oriented fragments of charcoal that are laterally continuous across the width of the thin section [mF B^2] (Table 4). Charred plant remains in mF B^1 are relatively smaller and more fragmented than in mF B^2, which may reflect remobilisation and trampling (Goldberg and Berna 2010). Microfacies B^2 may reflect *in situ* combustion or limited transport of combustion residues, resulting in preservation of large fragments. Arrangement patterns of carbonised residues in mF B^1 range from random and unoriented which confer a chaotic aspect to the deposits (Fig. 4f), to horizontally-oriented, fine laminations with embedded 'stringers' (Fig. 4g, Table 4) and *in situ* crushing of inclusions. The unstructured, unoriented units suggest rapid dumping of materials whereas the laminated, horizontally-oriented units could have formed through a combination of hearth rake-out activities involving the lateral redistribution of components in outdoor midden areas, followed by subsequent trampling/traffic on external surfaces (Rentzel and Narten 2000; Miller et al. 2010; Aldeias et al. 2012: 2418; Milek 2012; Mallol et al. 2013; Mentzer 2014; Mallol et al. 2017; Rentzel et al. 2017; Villagran et al. 2017b; Karkanas and Goldberg 2018). As in mF A, evidence for wetting of the sediments following deposition (decalcification of ash, Fe-Mn mobilisation), and subsequent reestablishment of dry conditions (precipitation of authigenic gypsum in lenticular crystal

---

[2] K diatoms/g sed = thousands of diatoms per one gram of sediment.

intergrowths, Fe-Mn precipitation, organic matter decay, soil faunal excrements and bioturbation features) indicate fluctuating wetting and drying conditions typical of an outdoor area.

In both mF A and mF B, redeposition of combustion residues is suggested by the unstructured microfabrics; random distribution of unsorted coarse components; lack of rubified substrates and tripartite microstructures of intact combustion features; and, the absence of intrusive materials (Fig. 4, Table 4; Aldeias et al. 2012: 2418; Mentzer 2014; Mallol et al. 2017; Villagran et al. 2017b). Occasionally, calcitic ash rhomb pseudomorphs of calcium oxalate crystals are preserved in anatomical position within carbonised plant remains. These features are not consistent with thin lenses of articulated ashes that Mentzer (2014) and Villagran et al. (2017b) attribute to intact combustion features. Nevertheless, the fragility of ashes implies low reworking and/or short distances of remobilisation (Mentzer 2014; Villagran et al. 2017b: 27). Thus, the formation of mFs A and B is linked to site maintenance practices involving the burning of large amounts of plant waste, followed by the collection of residues from the scene of combustion and secondary dumping in an outdoor midden area. Microfacies A and B are the most common microfacies and their repetition throughout the stratigraphic sequence indicate that burning and waste management were deliberate, routine practices. Burning may have been performed for sanitation purposes (e.g., to reduce odours and pests) and/or to reduce volume of waste deposits (Goldberg et al. 2009; Miller and Sievers 2012). Microfacies A and B are consistently compacted and occasionally show horizontal orientation of components and laminated microfabrics, implying that middens also functioned as external surfaces for traffic and activities.

4.2.2. MICROFACIES C : CLAY PLASTER FLOOR SURFACES

Clay plastered surfaces [mF C] are identified as thin layers 1-2 cm in thickness of relatively pure silty clays that were intentionally laid to create extensive surfaces (Fig. 6). The silty clays were deliberately applied wet to the substrate, producing well-oriented clay domains (Fig. 6c-6d) and strong horizontal orientation of inclusions (Fig. 6d-6e). The absence of reddening in thin section (Fig. 6) and the FTIR composition of unaltered clays (Fig. 5a, Table 4) indicate that the clays are not burnt. The sharp boundaries, well sorted texture and purity of the silty clay fabric (Fig. 6a-6c), lack of graded bedding typical of waterlain deposits, and the presence of anthropogenic inclusions (well-sorted, infrequent microscopic fragments of charcoal, burnt and unburnt bone and phytoliths) (Fig. 6d) indicate an anthropogenic rather than natural depositional process. Phytolith extraction revealed moderate phytolith (491-1,016 K phyt/g sed[3]) and elevated diatom (982-4,106 K diatom/g sed) concentrations (Table 4, Fig. 7). Similarities in clay fabric and inclusions (e.g., diatoms, sponge spicules and quartz silts and sands) with archaeological ceramics from the site and modern local clays from Lo Gach village suggest the probable use of local clays containing concentrations of diatoms (Fig. 6f). Dislodged aggregates occurring along the upper boundaries could have formed through sweeping and/or trampling (Matthews and Postgate 1994: 190; Matthews 2005) while planar fissures which characterise the microstructure of mF C (Fig. 6a) could have formed through trampling and/or post-depositional desiccation (Ge et al. 1993; Rentzel and Narten 2000; Milek 2012: 126; Rentzel et al. 2017). In some contexts [H1_9.3, H2_2.2], mF C occurs as disaggregated and displaced concentrations of sub-angular clay plaster fragments and plant-tempered clay construction aggregates (Fig. 6g-6h), suggesting dumping of construction materials from the levelling of old surfaces (Courty et al. 1994: 12; Shillito and Matthews 2013: 695).

---

[3] K phyt/g sed = thousands of phytoliths per one gram of sediment.

4.2.3. MICROFACIES D: DEPOSITION OF RICE PROCESSING BY-PRODUCTS

Microfacies D consists of articulated phytoliths and silicified plant fibres in anatomical connection and arranged in a laminated microstructure (Fig. 8f, Table 4), suggesting *in situ* decay of plant remains (Shillito et al. 2011a: 1030). FTIR analyses returned spectra dominated by opal (phytoliths) and gypsum (Fig. 5d, Table 4), and phytolith concentrations reported elevated phytolith values (2,257 K phyt/g sed) (Fig. 7, Table 4). Similar deposits composed of finely laminated, articulated phytoliths have been reported at other archaeological sites, where they have been interpreted in a number of ways, including: plant materials for bedding, followed by deliberate burning as part of site maintenance at Palaeolithic deposits at Sibudu Cave, South Africa (Wadley et al. 2011), supported by an experimental study (Miller and Sievers 2012); crop processing waste at Neolithic Catalhoyuk, Turkey (Shillito and Matthews 2013) and Neolithic Swifterbant, the Netherlands (Huisman and Raemaekers 2014); cereal processing storage features at Neolithic Goytepe, southern Caucasus (Kadowaki et al. 2015) and the middle Holocene agropastoral site of Loteshwar in India (Balbo et al. 2015); and, in the presence of faecal spherulites, burnt stabling material derived from dung in Iron Age deposits at Tel Dor (Shahack-Gross et al. 2005; Albert et al. 2008) and Tel Megiddo (Shahack-Gross et al. 2009).

In the phytolith-rich layers at Lo Gach, the dominant identifiable components are parts of rice plants, including mostly husks and some culms (Fig. 8e-8h), by-products of rice processing. Field excavation established that the layers were laterally extensive, covering several metres of the excavation trench and effectively ‘blanketing’ former midden surfaces (Fig. 8a). The undulating, sloping nature of the deposits (Fig. 2, Fig 8a-8b) is consistent with midden waste dumps and spreads (Albert et al. 2008: 73; Shahack-Gross et al. 2009: 175; Karkanas and Goldberg 2018) rather than an isolated feature such as a storage pit (Balbo et al. 2015; Kadowaki et al. 2015). There is an absence of dung indicators, such as faecal spherulites, amorphous organic matter or ingested, finely comminuted plant remains (Shahack-Gross 2011; Milek 2012; Shahack-Gross 2017; Karkanas and Goldberg 2018). Microfacies D is therefore interpreted as the remains of rice processing waste.

Rice processing involves three steps: first, threshing to remove the edible part of the rice from the rest of the plant, and this often takes place near the rice field; second, dehusking of the threshed components using a mortar and pestle; and, third, winnowing of the pounded rice to separate the grains from husks and other impurities (Cobo-Castillo 2018). The second and third steps usually take place at the habitation site. The plant remains in mF D are consistent with by-products produced in the second and third steps. During field excavation, circular depressions [F-111, F-112, F1-124, F1-131, and F1-132] (Fig. 8b-8c) were recorded in association with the phytolith layers. The circular depressions have striking parallels with mortar and pestles used to dehusk rice ethnographically in MSEA (compare Fig. 8b-8c this article with Cobo-Castillo 2018: 6459 Figure 2d-2e) and could be impressions formed from where the mortars sat. The sheer volume of plant remains contained in mF D and the recurrence of this microfacies within the stratigraphy suggest that intensive rice cultivation took place locally and rice processing formed a major activity in the locality of Trench 1. Occasional well-sorted quartz silt and sand lenses interbedded with phytolith layers (Fig. 8g) possibly represent syn-depositional natural inclusions from the local environment, suggesting unroofed spaces.

Following deposition, rice processing remains were heavily trampled, indicating traffic and activities in the outdoor space. Trampling is indicated by several micromorphological attributes, including: the finely laminated, compacted, undulating microstructures showing evidence of deformation from being pushed into the substrate (Fig. 6g-6h, Fig. 8f-8h; Shahack-Gross et al. 2005; Wadley et al. 2011); horizontally-oriented components and ‘stringers’ of bone, charcoal and organic material

(Table 4, Fig. 8h; Goldberg and Whitbread 1993; Rentzel and Narten 2000; Goldberg et al. 2009; Miller et al. 2010; Milek 2012; Rentzel et al. 2017); and, *in situ* crushing of bone and charcoal and *in situ* snapping of silicified plant fibres (Fig. 8h) (Miller et al. 2010; Villagran et al. 2017a: 26-27).

4.2.4. *IN SITU* BURNING EVENTS WITHIN MICROFACIES D

Two types of feature in the Lo Gach thin sections provide unequivocal evidence of *in situ* burning of plant waste. The first is a horizontally-oriented feature that extends across the width of the slide [MSU H1_4.8]. It contains calcitic pseudomorphs after calcium oxalate crystals aligned in anatomical position of the original plant structure and in parallel arrangement with carbonised tissues (Fig. 9c). Calcitic ash pseudomorphs are brittle, and this arrangement in plant anatomical structure would not have preserved if it had been redeposited from the place of combustion (Mentzer 2014).

The second type of feature comprises finely laminated layers of phytolith-rich plant remains dominated by rice husks [mF D] that show a microstratigraphic gradation in colour from a carbonised (black) base unit to an ashed (white-grey) top unit [H1_6.5] (Fig. 9a). This change in colour relates to the different temperature and conditions of a fire. The base of a fire has lower temperatures and is oxygen-depleted, inducing carbonisation, whereas the upper parts of a fire burn at a higher temperature and there is more available oxygen, inducing ashing (Goldberg et al. 2009: 111; Wadley et al. 2011). Gradations in colour of phytolith layers are interpreted as *in situ* combustion events in archaeological deposits (Goldberg et al. 2009; Wadley et al. 2011). *In situ* burning within mF D [MSU H1_6.5] may be a deliberate action linked to management of rice processing waste, such as for sanitation or to reduce the volume of waste (Goldberg et al. 2009; Miller and Sievers 2012). In another instance [MSU H1_1.5], the vertical sequence is switched so that the carbonised layer is on top and the ashed layer is on the bottom, and this reversed microstratigraphic sequence is repeated four times (Fig. 9b). The reversed microstratigraphy may represent repeated hearth sweeping and rake-out activities.

4.2.5. MICROFACIES E: CULTURAL WASTE DUMPS IN TRENCH 2

Deposits in Trench 2 (Phases I and II) are grouped into mF E and were formed through midden deposition (Fig. 10). In contrast to thinly bedded midden layers in Trench 1, Trench 2 deposits are thicker layers of midden discard that are internally homogenous and lack laminated structures (Fig. 10). The Trench 2 deposits contain unsorted, randomly-oriented and admixed anthropogenic components characteristic of midden deposits (Fig. 10; Courty et al. 1989: 118; Matthews et al. 1997: 289; Graham et al. 2015: 16). Anthropogenic inclusions consist of charcoal (Fig. 10b), bone (Fig. 10b-10e), rice husks (Fig. 10d, Fig. 10f), melted phytolith slags (Fig. 10b), phytoliths (Fig. 10b, Fig. 10f, Table 4), pottery fragments, and clay plaster fragments. The inclusions range from microscopic particles embedded in the micromass to large fragments up to 4.5 cm (Fig. 10). The only evidence for *in situ* activities is trampling (*in situ* crushing of horizontally-oriented bone fragments) and it occurs only at interfaces between units [e.g., MSUs H2_5.1-5.2 and H2_6.1-6.2] (Fig. 10e), implying traffic took place on exposed surfaces during pauses in midden deposition.

Microfacies E sediments show high concentrations of phytoliths and silicified plant residues as well as bone and charcoal fragments (Table 4, Fig. 10). Compositional analyses indicate moderate to elevated phytolith concentrations (264-2,426 K phyt/g sed) (Table 4, Fig. 7) and an FTIR composition of altered (heated) clay, unaltered clay, quartz, CHAP and opal (phytoliths) (Table 4). Following deposition, mF E sediments have been intensively finely comminuted, reorganised and homogenised into soil peds by soil fauna, creating channel, sub-angular blocky and local biological granular microstructures (Fig. 10) and several types of biological pedofeatures including fabric packing, root sections, and excremental infillings.

Differences in the nature of the groundmasses and embedded coarse inclusions of the peds allow differentiation of Trench 2 sediments into three subvariants of mF E that reflect different human activities. Microfacies E^1 has high concentrations of microscopic charcoal, phytoliths and vesicular silica slags, conferring a grey (PPL) aspect to the fine material (Table 4, Fig. 10b) and indicating the burning of plant material. Microfacies E^2 is distinguished by a dotted, dark brown (PPL) amorphous organic micromass and high concentrations of burnt and unburnt bone fragments (Table 4, Fig. 10c), indicating animal processing and food preparation activities. The mixture of burnt and unburnt bone (micromorphology, Fig. 10c) and altered and unaltered clay (FTIR, Table 4) suggests exposure to different temperatures within a fire, or alternatively the mixing of residues with different pre-depositional pathways (Schiegl et al. 2003; Matthews 2005: 386; Villagran 2014: 216). Microfacies E^3 is characterised by a pale cream (PPL) micromass with a composition of rice husks, phytoliths, abundant small rounded and weathered bone fragments, and phosphatic features, indicating a combination of plant and animal waste (Fig. 10d, Fig. 10f). The abundance of leached, possibly digested bone (pale with a loss of internal structure in PPL; loss of birefringence in XPL; Villagran et al. 2017a: 31) and phosphatic pedofeatures associated with amorphous and fibrous organic matter, phytoliths, and neoformed needle-shaped crystals exhibiting high-order birefringence (possible authigenic phosphate minerals; Karkanas et al. 2000; Karkanas and Goldberg 2010) (Fig. 10f) indicate mF E^3 possibly derives from faecal waste (Karkanas and Goldberg 2010; Shillito et al. 2011b; Macphail 2017; Macphail and Goldberg 2017).

4.3. POST-DEPOSITIONAL PROCESSES

Post-depositional transformations are intensive in the tropics due to high temperatures and moisture levels that are conducive to biological productivity and chemical reactions (Friesem and Lavi 2017; Morley and Goldberg 2017). At Lo Gach, the effects of bioturbation are clearly seen in Trench 2 deposits where intensive invasion by soil fauna in addition to physico-chemical processes resulted in complete transformation of microstructures and intensive comminution of archaeological components resulting in pedogenic aggregates characteristic of mF E (Fig. 10).

Percolating solutions from saturation and a rising water table caused by seasonal heavy rains trigger two main processes of chemical diagenesis in Lo Gach sediments. First, water acts as a catalyst for calcite dissolution in calcitic ash deposits [mF A^1], leading to recrystallised, indurated calcitic masses (Fig. 4a, Fig. 4c, Fig. 11b-11c) (Karkanas et al. 2007). The dissolution of calcitic ashes and bones is promoted by acidic conditions in tropical burial environments (Friesem and Lavi 2017) with bioerosion by microbial action also a possible factor (McAdams et al. 2020). Lo Gach deposits have a pH of ~7-8 (Table S4.4); localised acidic conditions are indicated by the dissolution of calcitic ashes which takes place below a pH of ~8 (Weiner 2010: 172) and leaching of bone (Fig. 11f) which is stable above a pH of ~7.6 but dissolves at lower pHs (Berna et al. 2004). Dissolution also produces physical effects on microfabrics in the form of vughy and compacted collapsed microstructures (Fig. 11c). Second, iron and manganese oxide precipitation result from redoximorphic processes associated with alternating wetting and drying cycles (Lindbo et al. 2010), resulting in the precipitation of neoformed oxide minerals (Fig. 4c-4f, Fig. 11c-11e, Fig. 11j). The solubility of iron and manganese increases with decreasing pH, thus acidic environments tend to experience greater movement of iron and manganese (Karkanas et al. 2000: 920). On the other hand, localised alkaline conditions buffered by calcitic ashes is indicated by infillings of phosphatised secondary clays and iron within internal charcoal structures (Fig. 11i) (Huisman et al. 2012). The prevalence of chemical reactions triggered by the alternating presence and absence of water suggest that most deposits excavated at Lo Gach were probably uncovered and therefore exposed to the weather. In this environment, the observation of diatoms in the sediments (Fig. 7) may reflect autochthonous growth during a period of wet saturated conditions at the site (see Grono et al. 2022).

In addition to fluctuations in the water table, Fe and Mn precipitation can also result from past reducing conditions created by the destruction of organic materials (Karkanas et al. 2000: 920). Organic matter decay requires and consumes available oxygen resulting in locally reducing conditions that in turn promote the movement of iron and manganese (Karkanas et al. 2000: 920). Extensive organic matter decay in the Lo Gach sediments constitutes a secondary pathway for iron and manganese mineral oxide formation. Fe and Mn are observed to replace organic matter, often as pseudomorphs preserving the original outlines of the organic material (Fig. 11g-11h) and around plant shrinkage voids containing decayed or combusted plant tissues (Fig. 11d) (Macphail and Goldberg 2010, 2017: 202, 296; Banerjea et al. 2015a: 108; Friesem et al. 2016: 21; Karkanas 2017: 134-137).

Two main chemical elements are released during the decay of organic matter: phosphorous and sulphur (Weiner 2010: 58). Phosphorous is detected in the Lo Gach sediments in the form of phosphatised groundmasses containing carbonised tissues [mF B^1] and phosphatised ashes [mF A^1] (Fig. 4d, Fig. 11j) and is supported by the identification of CHAP by FTIR (Table 4). Phosphate does not generally travel far from the site of dissolution and is an indication of large amounts of organics decaying *in situ* (Karkanas 2017: 133). Sulphur is oxidised to sulphate in aerobic conditions and binds to cations to produce authigenic minerals such as gypsum (Weiner 2010: 59), which is widespread in the Lo Gach sediments (Fig. 8j-8k). Gypsum precipitation requires sources of calcium (e.g., released from calcitic ashes, plant matter and bone) and sulphur (released through the decay of large amounts of organic matter and/or animal residues) (Weiner 2010; Milek 2012: 130). Oxidation of sulphur creates an acidic environment leading to the breakdown of phosphate-bearing materials such as bone and organics, and the release of calcium from dissolution of calcitic ash and bones. Calcium and sulphate then precipitate out of solution in the presence of oxygen to form gypsum. Authigenic gypsum has been identified in many archaeological contexts where it has precipitated from different sources of degrading organic matter including animal stabling deposits (Milek 2012; Shahack-Gross 2017); crop storage features (Kadowaki et al. 2015); and, the degradation of human bodies (Bergada et al. 2015).

In the Lo Gach sediments, lenticular gypsum intergrowths are extensive in the phytolith-rich layers of mF D, where the gypsum disrupts the finely laminated layers (Fig. 8j-8k). Goldberg et al. (2009: 11), Shillito et al. (2011a: 1030) and Kadowaki et al. (2015) describe the precipitation of gypsum within phytolith-rich layers resulting from the decay of plant materials *in situ*. According to Weiner (2010) and Milek (2012), gypsum is usually associated with drier conditions and rarely preserves in moist environments. Preservation of authigenic gypsum in Lo Gach deposits points to surprisingly good preservation conditions. The lenticular morphology of the gypsum crystals indicates relatively slow growth of mineral crystals requiring waterlogged conditions for some time. Gypsum precipitation probably occurred prior to the deposition of the overlying clay plastered surfaces (mF C) and its preservation was likely enabled by the impermeable clay surfaces which would have prevented moisture infiltration above and below the units in which gypsum occurs.

5. DISCUSSION

5.1. A MICROSTRATIGRAPHIC SEQUENCE OF SETTLEMENT HISTORY

Microarchaeological analyses established that most of the stratigraphy at Lo Gach comprises organic waste. Due to the dominant organic composition and the undulating, mounded and deformed bedding structures that are observed in profile (Fig. 2), the excavated part of the site is identified as an extensive area of midden dumping (Karkanas and Goldberg 2018: 141). A microstratigraphic sequence of site formation shown in Fig. 12 for Trench 2 and Fig. 13 for Trench 1 is based on the stratigraphic patterning of microfacies integrated with radiocarbon dating to thereby reconstruct the site history and use of space over time at Lo Gach. A handful of depositional activities (microfacies) repeated multiple times throughout site occupation are responsible for the accumulation of site stratigraphy. Archaeological components show consistency in respective depositional pathways, indicating that waste management is a highly regulated and structured practice that was repeated numerous times. The Bayesian chronological modelling suggests that these recurrent practices took place across a relatively short period of time (less than 220 years for Phase II), producing relatively rapid build-up of deposits.

The earliest archaeological layers at Lo Gach were deposited in Trench 2 between c. 3300-3000 cal. BP. Trench 2 comprises thick, homogenous layers attributed to midden dumping of materials generated by human activities: the burning of plant material [mF E^1: C.205 and C.204]; animal processing activities [mF E^2: C.205, F2-7, F2-13, F2-42 and F2-53]; and, plant (predominantly rice) and animal activities, possibly deriving from faecal waste [mF E^3: C.204 and C.202] (Fig. 10, Fig. 12). Rice remains are observed in thin sections from the earliest layers, indicating rice was present from initial occupation of the site (c. 3300-3000 cal. BP). In one thin section [MSU H2_2.2] from Trench 2, disaggregated aggregates of clay plaster represent dumping of construction debris (Fig. 12). The only *in situ* activities in Trench 2 is occasional trampling on exposed midden surfaces between dumping episodes (Fig. 10e). Unlike Trench 1 deposits, trampling on exposed midden surfaces was not intensive and it is presumed that Trench 2 was located further away from the contemporaneous habitation site than Trench 1 was during the later phase of occupation. The absence of the Phase I Trench 2 deposits in Trenches 1 and 3 to the west suggests that the 3300-3000 cal. BP settlement was either not as extensive as the later phase of occupation, or was located in a slightly different area of the site.

Trench 1 deposits date to a tightly constrained period between c. 2750-2400 cal. BP with deposition lasting no more than 220 years, implying relatively rapid build-up of the stratigraphy (Fig. 13). Microarchaeological analyses establish that Trench 1 deposits contain almost entirely anthropogenic sediments comprising thin, laminated layers of organic waste (Fig. 13). Midden accumulation was rapid and continuous, indicated by the sharp boundaries between different deposits, minimal pauses in deposition, and a lack of intrusive materials and natural clastic sedimentation (Shillito and Matthews 2013). Furthermore, many of the deposits recorded at Lo Gach represent single, sequential depositional events, suggesting the stratigraphic sequence likely records sediment accumulation over decades, rather than centuries.

Among the earliest cultural layers in Trench 1 was C.103, a silty clay plastered floor surface [mF C] 2-3 cm in depth and extending across the trench (Fig. 6, Fig. 13). Basal deposits at Lo Gach are permeable fine sands and it is therefore conceivable that local clays were deliberately mobilised to construct a hard, even and sanitised foundation surface for occupation. The plastered surface shows evidence of possible trampling and sweeping (Section 4.2.2). The construction of floor surfaces on middens has also been reported at Neolithic Catalhoyuk in Turkey (Shillito and Matthews 2013: 45).

Midden accumulation took place above the clay plaster surface, indicating that the locality subsequently reverted to a midden area (Fig. 13). Three midden deposit types are distinguished: ashes of woody and grassy plants [mF A] (Fig. 4a-4d); carbonised plant residues [mF B] (Fig. 4e-4f); and, silicified rice remains containing articulated phytoliths [mF D] (Fig. 8). The three midden types were deposited in alternating, finely stratified layers formed by discrete depositional episodes of midden building that were repeated numerous times, reflecting cyclic human activities around the settlement (Fig. 13; Huisman et al. 2009).

The frequent occurrence of the first two midden deposit types – ashes and carbonised plant remains – suggest that burning is a major site formation process at Lo Gach that utilised vast amounts of plant materials and involved deliberate, routine actions linked to site maintenance practices (Fig. 13). Occasional pinky and orange colours within these layers were attributed to heat alteration in the field, however, thin section analyses suggest that most burnt components are in redeposited contexts and that pinky-orange colours are a result of phosphatisation and redoximorphic processes related to post-depositional alteration of ashes (Section 4.3). Infrequent occurrences of *in situ* burning of midden waste (Fig. 9) indicate burning was undertaken to sterilise the deposit and reduce the amount of organic waste (Shahack-Gross 2011; Miller and Sievers 2012).

Excavations at Lo Gach produced large numbers of fragmented ceramic tripods identical to those recorded at Go O'Chua, a contemporaneous (in the later phase of Lo Gach) settlement site on the Vam Co Tay River close to the Vietnamese-Cambodian border (Bui et al. 2003; Bui 2008; Proske et al. 2009). The tripods have been interpreted as evidence for salt making using the briquetage method of heating saline water in small dishes supported by the tripods (Proske et al. 2009; however Vietnamese archaeologists have argued that the tripods were used in pottery manufacture as supports for drying newly constructed ceramics before firing). Sordoillet et al. (2018) describes an earlier, pre-briquetage method of salt making involved pouring brine on hot embers, a method which produces large amounts of combusted plant remains. Micromorphology studies from early Neolithic contexts in Romania (Sordoillet et al. 2018) and Late Classic period in Belize (Macphail et al. 2017) show concentrations of burnt plant remains in association with salt processing residues. Today, Lo Gach is approximately 125 km inland in a southeast-northwest direction from the coast; however, in the mid Holocene sea levels were higher than present (Nguyen et al. 2000; Ta et al. 2002; Stattegger et al. 2013) and as sea levels retreated a mangrove environment was established in the vicinity of the site (Proske et al. 2010). Saline water may thus have been an available resource nearby the site. We therefore raise salt making as a tentative interpretation for the production and deposition of some of the burnt plant layers at Lo Gach, in the context of the Go O'Chua salt making hypothesis and substantial material culture similarities between Lo Gach and Go O'Chua, but this hypothesis remains speculative.

The third midden deposit type comprises articulated phytoliths representing plant processing waste, predominantly silicified rice husks from dehusking rice [mF D] (Fig. 8). Rice cultivation and harvesting would have been a periodic behaviour. The rice layers were perhaps deposited during single events when the inhabitants of Lo Gach were processing rice, reflecting annual or seasonal rhythms tied to the agricultural cycle.

Deposition of the rice layers [mF D] may have been motivated by waste discard only. However, the purity of the phytoliths and silicified plant material (Fig. 8f) as well as the extensive 'blankets' of deposition that they form across the trench (Fig. 8a), suggest that the deposits may have provided a dry surface for activities such as sitting, resting or working (Goldberg et al. 2009) or thoroughfares for walking (Huisman et al. 2009). This would be particularly advantageous in the tropics where muddy substrates commonly last several months of the year. The sheer quantities and repeated occurrence of rice by-products in thin section indicates rice processing was a major activity performed at Lo Gach and that rice was likely a staple food for the inhabitants.

The undulating, mounded and deformed bedding structures observed in profile, primarily with a downslope from east to west (Fig. 2, Fig. 8a-8b, Fig. 13), are a result of a combination of three processes: uneven mound dumping and lensing related to the nature of midden deposition; trampling on exposed midden surfaces; and, post-depositional deformation and slumping due to volume reduction and self-compaction through *in situ* decay of organic matter and dissolution of calcitic ashes (Albert et al. 2008: 73; Shahack-Gross et al. 2009: 175; Karkanas and Goldberg 2018). Given that the stratigraphy contains mostly organic waste, reduction in volume of the deposits after burning and/or decay would have been significant and may have changed stratigraphic associations between deposits (Albert et al. 2008; Miller and Sievers 2012). A suite of post-depositional processes provide evidence for fluctuating wet (structural collapse, decalcification of ash, Fe-Mn mobilisation) and dry (precipitation of authigenic gypsum, Fe-Mn precipitation, calcite recrystallisation, phosphatisation, organic matter decay and soil fauna activity) conditions that would be expected in an outdoor area uncovered and exposed to the weather (Section 4.3). Periods of trampling and exposure of external surfaces between episodes of midden accumulation contributed to the laminated and undulating stratigraphy and portray a lively picture of an outdoor area that was utilised for a variety of activities related to plant processing, burning, and waste management.

5.2. A MICROSCALE WINDOW INTO MACROSCALE TRANSITIONS: THE EMERGENCE OF SEDENTISM AND AGRICULTURE IN MSEA PREHISTORY

Based on microarchaeological analyses, the excavated area is interpreted to be the ‘backyard’ of the settlement constituting an outdoor space that was used as thoroughfares and external surfaces for rice processing and waste management. Radiocarbon dating established an initial occupation of Lo Gach between c. 3300-3000 cal. BP, followed by the main occupation of the settlement between c. 2750-2400 cal. BP, a time period contemporaneous with the possible transition into the early bronze age in MSEA (see Higham and Cawte 2021). A hiatus in deposition may have occurred around 3000-2800 cal. BP (between Phase I and Phase II), however it cannot be determined whether this reflects site abandonment or a hiatus in localised use of space within the settlement. By Phase II, the phase which accounts for the main occupation of the settlement, cultural deposition was continuous, indicated by the absence of breaks in accumulation; intensive, indicated by persistent foot traffic and the rapid accumulation of cultural waste; and, highly regulated and systematic, indicated by the repeated deposition of specific material components (Fig. 13).

Amongst the waste deposits at Lo Gach are substantial amounts of rice processing by-products (Fig. 8) suggesting rice was cultivated locally. Considerable amounts of rice in sediments dating to c. 3300-3000 cal. BP (Phase I) indicate rice cultivation and consumption was practiced from the earliest phases of settlement occupation (Fig. 12). By Phase II (c. 2700-2450 cal. BP), regular deposition of dense accumulations of rice processing waste implies intensified cultivation and the development of routine practices of managing agricultural waste (Fig. 13). Evidence for agricultural intensification during the bronze age at Lo Gach supports regional evidence for the increasing reliance on domesticated plants and animals during the bronze age in Thailand (Higham 2014; O’Reilly 2014) and China (Flad et al. 2007; Cohen 2011). Taken together, these findings suggest agricultural production in MSEA intensified during the metal age.

Rice agriculture requires a degree of permanence in land use to accommodate routine planting and harvesting of crops, and synchronisation of the social rhythms of a community to the agricultural cycle (Barton and Denham 2011). Based on the evidence for intensive rice processing (Fig. 8), the continuous nature of cultural accumulation and a lack of natural sedimentation or breaks in the stratigraphy (Fig. 12-13), and the remains of domesticated dogs and pigs and commensal rodents recovered from the site (Tran and Piper 2018), Lo Gach was probably inhabited by a sedentary community involved in rice agriculture and animal management. Waste represents a ‘crisis’ (Rathje and Murphy 1992: 33; Hardy-Smith and Edwards 2004: 253) unique to sedentary communities, who must manage the continual accumulation of rubbish around habitation areas. At Lo Gach, site formation appears to have been motivated by the problem of waste. A change in waste disposal strategies is identified between the Trench 2 and Trench 1 deposits (Fig. 12-13). Trench 2 deposits contain thick, more homogenised layers with less evidence for individual *in situ* activities and less compaction from foot traffic (Fig. 10); Trench 2 was probably positioned on the periphery of the main areas of activity in the settlement. In contrast, Trench 1 deposits contain finely stratified layers of repeated activities and specific pathways of components, reflecting planning and regulation of waste management (Fig. 13).

While the 2014 excavation appears to have missed the main area of habitation and dwellings, several postholes dug into midden deposits possibly represent small outbuildings or lightweight structures that could have been used for such activities as storing grain or firewood. The use of perishable plant materials to construct dwellings is supported by woven mat impressions on surfaces (Fig. S1.1; Cameron 2017) and the abundance of plant remains identified in the Lo Gach sediments. The use of plant materials for construction is a common ethnohistoric practice in Southeast Asia (Bernot 1982; Waterson 1990) and may be a contributing factor for the lack of recognised prehistoric settlements the region (White and Eyre 2011: 62; Grono 2020).

At one point during Lo Gach's settlement history, local clays were applied as a plaster across an exposed midden to create an impermeable surface (Fig. 6). The production and maintenance of floor surfaces appear to be relatively common in the neolithic of Vietnam, having been recorded at An Son (4250-3150 cal. BP), Loc Giang (c. 3900–3230 cal. BP) and Rach Nui (c. 3500 to 3300 cal. BP) in Long An Province (Nishimura and Nugyen 2002; Piper and Oxenham 2014). The floor surfaces at the neolithic sites vary significantly from those recorded at Lo Gach, in that they were constructed using lime mortar, rather than clay (Grono et al. in press; Piper et al. 2017). In Thailand, hard floor surfaces from iron age Ban Non Wat (c. 2500-1500 cal. BP) are presumed to be living or working surfaces where domestic activities involving animal processing (Kanthilatha et al. 2014) and metal production (Duke et al. 2011) took place. Clay-lined floors have been described from metal age contexts at Ban Non Wat (Higham and Kijngam 2012), Non Ban Jak (Higham et al. 2014; Higham 2017), Non Yang (Nitta 1991) and Non Muang Kao (O'Reilly 1997), where they occur in proximity to human burials and are attributed a domestic or mortuary function. The floors in sites in Thailand have not been subject to micromorphological analysis, thus the technology of the floors or how similar they are to the Lo Gach plasters remains unknown.

Settlement and habitation areas are severely underrepresented in MSEA prehistory (Piper and Oxenham 2014; Higham 2017; Grono 2020). The findings reveal that evidence for settlements certainly exist in MSEA prehistory, however a contributing factor to their limited detection is the low archaeological visibility and preservation of habitation areas in tropical environments. The low visibility and preservation are a result of several factors, including the use of outdoor spaces, use of organic materials in construction, and destructive post-depositional processes (Grono 2020; Grono et al. 2022). The detection of settlement evidence is best achieved using microarchaeological techniques capable of identifying millimetric occupation layers and complex diagenesis pathways that are often hidden during field excavation. At Lo Gach, as at other tropical sites (Stephens et al. 2005; Lewis 2007; Simpson et al. 2008; Kourampas et al. 2009; Friesem and Lavi 2017), durable microscopic indicators of occupation such as phytoliths, charcoal, iron and phosphorous preserve in the sediments when many other types of archaeological remains have decayed. The results of the study also indicate that waste management strategies are one of the most detectable forms of settlement activity and, when studied at the micro-scale, offer high-resolution insights into economic and social practices.

6. CONCLUSION

Following initial occupation of Lo Gach between c. 3300-3000 cal. BP, the main occupation of the settlement took place sometime between c. 2750-2400 cal. BP. Microarchaeological investigations demonstrate that most of site stratigraphy comprises organic waste from rice processing and remobilised burnt plant material. Site formation was motivated by the problem of waste as inhabitants undertook structured site maintenance activities including systematic waste disposal in designated outdoor areas and *in situ* burning to reduce volume and sterilise deposits. Major and repetitive structural transformations generated from surface pressure attributed to trampling on the deposits indicate that midden areas functioned as external surfaces for traffic and activities. Intensive post-depositional processes encompassing the chemical dissolution and mobilisation of calcium carbonate, iron, manganese and phosphate and the authigenic precipitation of gypsum as well as bioturbation indicate that the deposits were generally uncovered and exposed to the weather. Microarchaeological analyses successfully disentangled the complex diagenetic transformations of stratigraphy to reconstruct a lively picture of an outdoor 'backyard' area of the prehistoric settlement that the inhabitants utilised for a variety of activities related to traffic thoroughfares, plant processing, burning, waste management, and site maintenance.

ACKNOWLEDGEMENTS

The 2014 archaeological investigations at Lo Gach were conceived and directed by Nguyen Khanh Trung Kien and Philip J. Piper as a collaboration between the Centre for Archaeology, Southern Institute of Social Sciences (Ho Chi Minh City), Long An Provincial Museum (Tan An) and the School of Archaeology and Anthropology, Australian National University (Canberra). The authors would like to thank the investigative team for all their hard work on the project: Le Hoang Phung, Nguyen Hoang Bach Linh, Nguyen Nhut Phuong, Nguyen Ngoc Hong, Van Ngoc Bich, Do Thi Lan, Tran Thi Kim Quy, Jasminda Ceron, Cristina Cobo-Castillo and Fredeliza Campos. The authors kindly acknowledge Adelaide Petrographics and John Vickers and Shane Paxton, Australian National University for assistance with thin section preparation; Ulrike Proske, Janelle Stevenson and Jack Fenner for laboratory access and support; the Geoarchaeology Research Group, Australian National University; and, the Kimmel Center for Archaeological Science, Weizmann Institute of Science for the online Library of Infrared Standards. The time and effort devoted by three anonymous reviewers to improving the quality of this manuscript is gratefully acknowledged. In addition, Elle Grono extends thanks to three anonymous thesis reviewers whose comments improved research presented here.

DECLARATIONS

The authors have no relevant financial or non-financial interests to disclose.

FUNDING

This research was funded by an Australian Government Research Training Program Scholarship (2015-2018) awarded to Elle Grono. The 2014 excavations at Lo Gach was funded by a small grant from the Research School of Humanities and Arts, College of Arts and Social Sciences, ANU awarded to Philip J. Piper and Nguyen Khanh Trung Kien.

AUTHOR CONTRIBUTIONS

All authors contributed to the study conception and design. Nguyen Khanh Trung Kien, Philip J. Piper and Dang Ngoc Kinh directed the field project and undertook field excavation, recording and collection of samples. Microarchaeological analyses were undertaken by Elle Grono with supervision from Tim Denham and David E. Friesem. Radiocarbon dating and Bayesian modelling was performed by Rachel Wood with assistance from Philip J. Piper. The first draft of the manuscript was written by Elle Grono with assistance from Rachel Wood and Philip J. Piper. All authors commented on previous versions of the manuscript and read and approved the final manuscript.

FIGURE CAPTIONS

Fig. 1 The location of Lo Gach in southern Vietnam, on the west bank of the Vam Co Tay River and near the Cambodian border

Fig. 2 Site map and excavation profiles of Lo Gach. (a) Profile of Trench 2 (*west wall*) showing major stratigraphic layers and features and the location of micromorphology blocks. (b) Site map showing the location of two trenches excavated in 2014 in relation to previous excavations, modern buildings, and the Vam Co Tay River. (c) Profile of Trench 1 (*west wall*) showing the thin, compacted and undulating nature of the deposits. Kubiena tins in the profile denote the location of some of the micromorphology blocks sampled from Trench 1. Additional blocks were sampled from the east wall (not shown here) Note differences in the nature and complexity of stratigraphy between Trench 2 (*top*) and Trench 1 (*bottom*)

Fig. 3 Calibrated and modelled ages (BP) within the 95% probability range for the Trial Trench and Trenches 1, 2 and 3 at Lo Gach using the Charcoal Plus Outlier Model (Model B). Chronological sequences present the oldest dates in each trench at the bottom of the model (all the samples are charcoal unless otherwise stated)

Fig. 4 Compacted midden deposits composed of ash residues representing mF A (a-d) and carbonised plant residues representing mF B (e-f). (a)-(d) Compacted, indurated calcitic ash deposits of mF A containing frequent coarse inclusions of charcoal and vitrified phytolith slags. The coarse inclusions are arranged in a random and chaotic microstructure indicating a rapid, single event of deposition. The fine material varies from crystallitic (XPL) microcrystalline calcite (shown in b) to cryptocrystalline pale orange (PPL) mottled isotropic (XPL) phosphatised ashes (shown in d). The deposits are also variably stained with dendritic Fe-Mn oxides (shown in c and d). (e) Carbonised plant residues of mF B^1, containing abundant carbonised rice husks indicating burning of rice processing by-products. (f) and (g) show two types of arrangements of carbonised plant residues that are common in mF B^1: (f) poorly-sorted carbonised plant remains showing a random and chaotic arrangement within a cryptocrystalline pale orange (PPL) isotropic (XPL) phosphatised groundmass; and, (g) strands and ‘stringers’ of charred plant fragments, amorphous organic matter and phosphatised fine material arranged in horizontally-oriented laminations

Fig. 5 Representative Fourier-transform infrared (FTIR) spectra showing common mineral compositions of sediments from Lo Gach. For all FTIR mineral identifications and representative spectra collected on sediments from the site refer to Supplementary Material 4. (a) Spectra of unaltered clay (indicative peaks along the main clay O-H region 3400-3700 cm^{-1}, the main Si-O stretching band at 1033 cm^{-1} and at 1012, 913, 532 and 468 cm^{-1}) and quartz (shoulder at 1084 cm^{-1}, peak at 695 cm^{-1} and doublet at 798 + 778 cm^{-1}). This spectra is representative of the clay plastered surface of mF C. (b) Spectra of altered (heated) clay, showing an upward shift of the main Si-O band (to 1035 cm^{-1}), diminishing of absorption bands in the O-H region (3600s cm^{-1}) and disappearance of the shoulder at 1012 cm^{-1} and peak at 913 cm^{-1}, changes which result from the loss of structural water in the clay minerals (dehydroxylation) (O-H region) and conversion of clay minerals to amorphous and crystalline phases (Si-O) region. Spectra containing altered clay was common to all sediments excepting mF C which contained non-altered clay. (c) Spectra of altered (heated) clay (note similarities with (b)) with additional constituents of calcite (indicative absorption bands at 1484, 858 and 713 cm^{-1}) and aragonite (indicative absorption peaks at 1484, 879 and 713 cm^{-1}). This spectra was common in deposits containing ashed and combusted plant residues of mF s A and B, suggesting the calcite and aragonite are likely to be pyrogenically-formed from the exposure of plant materials to temperatures exceeding 600°C. (d) Spectra of amorphous silica (opal) (indicative absorption peaks at 1098, 800 and 473 cm^{-1}). Opal is present in a biogenic form (plant silica of phytoliths) and is a major constituent of the laminated layers of phytoliths and rice processing waste deposits of mF D. Plant silica is also a constituent in other microfacies including the midden deposits of plant materials, mFs A, B and E

Fig. 6 Photomicrographs of mF C, representing clay construction technologies at Lo Gach. (a)-(e) Clay plastered surfaces. The clay is relatively pure and the well-oriented clay domains (parallel-striated b-fabric) in (c) and (d) and horizontal orientation of infrequent inclusions in (d) and (e) indicate a wet, plastic state of application. Vesicles shown in (b) formed through trapped air during floor mixing and pugging. Planar cracks shown in (a) may represent desiccation cracks from drying or pressure cracks from trampling and/or sweeping. (b) Infrequent anthropogenic components in (d) include microscopic unburnt and burnt bone fragments and charcoal particles and are probably incidental inclusions. The clay contains abundant diatoms, shown in (e), similar to local clays nearby the site. (f) Geoethnoarchaeological sample of a modern clay floor from Lo Gach village, showing use of local clays containing abundant diatoms and sponge spicules. (g) A clay construction aggregate showing a well-pugged fabric and internal vughs and vesicles from the addition of plant materials and/or trapped air. The clay aggregate is in a displaced, secondary context within trampled sediments that have been pressed into undulating laminated arrangements. (h) Magnification of the rectangle shown in (g), showing the effects of trampling on sediments surrounding the clay aggregate. Finely laminated sediments composed of articulated phytoliths and siliceous plant fibres appear pressed into the surface of the clay aggregate

Fig. 7 (a) Phytolith and diatom concentrations in archaeological deposits from Lo Gach, depicted according to microfacies groups. The microstratigraphic units sampled for biogenic silica concentrations are indicated in parentheses. The corresponding values are provided in Supplementary Material 4. Despite micromorphological analyses establishing that most of the deposits comprise plant material, the phytolith concentrations, while relatively elevated, do no greatly exceed the potential range of phytoliths in natural tropical soils. For example, mF D almost exclusively comprises silicified plant remains (Fig. 8) yet reported phytolith concentrations of less than 2.3 million/g of sediment. Common vesicular silica slags, shown in (b), derive from the melting of phytoliths at high temperatures (Canti 2003) and may account for relatively low phytolith concentrations. (b) *Left:* silica slag observed in a micromorphological thin section. *Right:* a silica slag following phytolith extraction

Fig. 8 Field stratigraphic features (a-e) and micromorphological attributes (f-k) of deposits containing rice processing waste. (a)-(e) Stratigraphic features containing rice remains recorded during excavation. (a) Photograph in plan view of an example of one of the white silicified 'rice blanket' layers [F1-126] comprising almost exclusively of silicified rice husks. (b) Example of a hard, compacted surface [F-110] on which rice processing activities were taking place, showing a circular depression, magnified in (c). (c) A circular depression [F1-111] identified on a hardened surface [F1-110] (see also Cobo-Castillo 2018: 6459 Figure 6c). The impression was possibly formed by a mortar and pestle used to dehusk rice similar to those used ethnographically in the region today (compare to Cobo-Castillo 2018: 6467 Figure 2d-2e). Field photographs provided by the Lo Gach archaeological team. (d) Macroscopic image of an intact fragment of a hard, compacted deposit packed full of rice chaff. The image also shows clay and iron enrichment on the surface of the rice chaff. (e) Silicified rice remains impressed onto a surface [F1-12]. (f)-(k) Photomicrographs of mF D, representing deposition of rice processing waste. (f) and (g) mF D^1 is comprised almost exclusively of elongate siliceous plant fibres, predominantly rice husks, arranged in a finely laminated and compacted, horizontally-oriented to undulating microstructure. (g) lenses of detrital silt and fine to medium sand quartz mineral grains represent syn-depositional aeolian inclusions, suggesting exposure in an outdoor space. (h) The effects of trampling can be seen in the *in situ* snapping of plant fibres. (i) Bioturbation occasionally disrupts the finely laminated, horizontal arrangements and results in the fine comminution of residues into excremental microaggregates. (j) Several clusters of authigenic lenticular gypsum crystals disrupt the finely laminated deposit by pushing the sediments at all angles. (k) A lenticular crystal intergrowth of gypsum

Fig. 9 Examples of microstratigraphic associations between ashing and charring. (a) Deposits of mF D^3, comprising siliceous and carbonised plant fibres, predominantly rice husks. There is a gradational change from charred (blackened) plant residues in the lower part of the image to ashed (grey) plant residues in the upper part of the image, indicating *in situ* burning. (b) Deposits of mF D^3; however, in this instance the microstratigraphic association is reversed, so that ashed (grey) plant residues are on the bottom and carbonised (blackened) plant residues are on the top. This association is repeated four times indicating a repeated depositional practice. The reversed stratigraphy is unlikely to represent *in situ* burning and instead may represent hearth sweeping and rake-out activities. (c) calcitic ash pseudomorphs after calcium oxalates in plant anatomical position showing parallel arrangement with charcoal fragments, indicating *in situ* burning. The remains may represent a single burnt plant fragment or possibly discarded, burnt matting

Fig. 10 Photomicrographs of mF E, representing occupation deposits in Trench 2. (a) A biological microstructure in which the fine and coarse fractions containing anthropogenic materials have been combined and homogenised into granular and subangular blocky peds by soil faunal activity. (b), (c) and (d) Three subvariants of mF E are identified based on differences in composition of the peds. (b) Subvariant mF E^1 is distinguished based on the abundance of microscopic to coarse charcoal fragments and siliceous plant materials including phytoliths, rice husks and vitrified phytolith slags embedded in the micromass. (c) Subvariant mF E^2 is distinguished based on two main attributes: the dark colour of the fine material that results from an abundance of amorphous organic matter; and, high concentrations of mixed burnt and unburnt microscopic bone fragments embedded into the micromass. (d) Subvariant mF E^3 comprises predominantly of rice husks and siliceous plant fibres with frequent unburnt, weathered bone fragments. (e) *in situ* fragmentation of bone indicating surface pressure (trampling). This type of feature occurs at the interfaces (stratigraphic boundaries) between different deposits. (f) Phosphatic features, common in mF E^3, possibly representing faecal waste. They contain leached bone fragments, siliceous plant materials including rice husks, fibrous dark brown (PPL) organic tissues (possible wool or fur), and authigenic, possibly phosphatic, crystals (XPL)

Fig. 11 Photomicrographs of post-depositional features relating to alternating wet and dry conditions and chemical diagenesis of anthropogenic materials. (a) Biological pedofeatures from soil faunal activity during dry and stable periods of burial. *Left:* original microstructures are completely transformed into homogenous, porous granular fabrics composed of finely comminuted materials and excremental aggregates. *Right:* biological features locally disrupt otherwise preserved microstructures, for example a biological void infilled with excremental microaggregates within a deposit that is otherwise compacted. (b) and (c) Indurated and recrystallised calcitic plant ashes, transformed by water saturation. (b) Calcitic ashes show loss of a grey micritic texture and rhombic morphologies typical of fresh ash, and exhibit recrystallisation into relatively pure microcrystalline calcite. The deposit has lost structure and has been compacted. (c) A calcitic groundmass showing collapse of structure into a vughy fabric. Fe-Mn oxide coatings on voids also attest to the presence of water. (d) Dendritic iron and manganese oxide hypocoating around a plant shrinkage void. (e) Intensive Fe-Mn oxide precipitation in a cryptocrystalline pale orange (PPL) isotropic (XPL) phosphatic groundmass containing charred plant remains. Fe-Mn oxide precipitation concentrates around the plant residues. (f)-(i) Processes involving the chemical alteration of organic and biomineral materials. (f) A bone fragment showing dissolution. (g) A pseudomorph of a rice husk showing complete replacement by iron oxide. (h) Replacement of organic material by iron oxides, showing diffuse impregnation at the edges of the material. (i) Infillings of clay, iron oxides and possible phosphatisation in charcoal fragments. (j) Phosphatisation and Fe-Mn oxide impregnation of massive ashes. Phosphatic enrichment presents as pale orange (PPL) isotropic (XPL) cryptocrystalline fine material

Fig. 12 Summary of the microstratigraphic sequence of Trench 2, Lo Gach, integrating field stratigraphy and radiocarbon dates with results from the microarchaeological analyses. Select thin section scans and photomicrographs are displayed to illustrate major deposit types and their stratigraphic patterning. Conventional radiocarbon ages have been calibrated in OxCal 4.4 (Bronk Ramsey 2009a) against a 50:50 mixture of the IntCal20 (Reimer et al. 2020) and SHCal20 (Hogg et al. 2020) calibration curves and quoted at 95.4% probability, rounded to ten years (see Table 1)

Fig. 13 Summary of the microstratigraphic sequence of Trench 1, Lo Gach, integrating field stratigraphy and radiocarbon dates with results from the microarchaeological analyses. Select thin section scans and photomicrographs are displayed to illustrate major deposit types and their stratigraphic patterning. Conventional radiocarbon ages have been calibrated in OxCal 4.4 (Bronk Ramsey 2009a) against a 50:50 mixture of the IntCal20 (Reimer et al. 2020) and SHCal20 (Hogg et al. 2020) calibration curves and quoted at 95.4% probability, rounded to ten years (see Table 1)

Table 1 Summary of major stratigraphic contexts and features at Lo Gach, listed with associated radiocarbon dates, attributed cultural phases, and micromorphology samples

Trench	Cultural phase	Dates cal. BP^	Context	Sediment description, archaeological associations and field hypothesis	Micromorph-ology blocks
1	Modern		C.100	Very dark grey (10YR 3/1) silt loam surface deposits consisting of modern topsoil with mixed archaeological and modern materials.	-
			C.101	Very dark brown (10YR 2/2) sandy loam deposits containing pottery sherds and fragments of compacted surfaces, displaced by modern activities.	-
	Phase II		C.102	Brown (10YR 4/3) loose sand deposit associated with the compacted surface deposits. Shows patchy distribution and contains ashy sediments, pottery sherds, faunal bones, discrete burning areas and fragments of displaced compacted surfaces.	H1_13
			F1-28	A series of compacted deposits recorded by feature number (F-#) comprising hard, compacted light brown (7.5YR 5/2) to yellow (10YR 7/6) surfaces composed of friable loamy sands, underlain by very dark grey (5YR 3/1) to black (10YR 2/1) organic and humic sediments rich in charcoal, ash and reddish-brown (5YR 5/3) burnt clay. Pottery, burnt clay, silicified rice remains, and leaf and woven matting impressions were occasionally visible in and/or on the surfaces.	F1-28
			F1-32		F1-32
			F1-61		H1_13
			F1-66		14LGaH1_13
			F1-80		H1_12
			F1-85		H1_10, H1_11, F1-85
			F1-91		F1-91
			F1-108		H1_7
			F1-109		F-109a: H1_5, F-109b: H1_5, H1_6
		2720-2370	F1-110		H1_5, H1_6
			F1-113		H1_4, H1_6
			F1-125		H1_3, H1_4
		2750-2490	F1-123		H1_2, H1_3
			F1-127		H1_2
			F1-140		H1_2
			F1-141		H1_1, H1_8, H1_9, F1-141
			F1-119	Stratigraphically alternating with the compacted surfaces were laterally continuous, thin (<3 cm) 'blanket' deposits of silicified plant remains (predominantly rice husks), ash and burnt organics (Fig. 8a). The layers were associated with circular impressions thought to have been formed through use of heavy rice pounders on the surfaces (Fig. 8b-8c).	H1_4
		2730-2490 [F1-121]	F1-122		H1_3, H1_4
			F1-126		H1_2
			C.103	Grey (5YR 6/1 to 5/1) silt loam homogenous deposit hypothesised to have been deliberately imported as a foundational floor surface. The initial compacted surface deposits (F1-141, F1-140) lie directly on top of C.103.	H1_1, H1_9
			C.104	Very dark grey (5YR 3/1) loose loamy sand containing charcoal, ash, faunal bones and pottery.	H1_1
		2850-2750	C.105	Dark brown (7.5YR 3/2) loose sand deposit containing pottery and faunal bones.	-
	Sterile		C.106	Grey (2.5Y 6/1) natural alluvial loamy sands, culturally sterile.	-
2	Modern		C.200	Dark brown (7.5YR 3/2) to dark greyish brown (10YR 3/2) sandy loam to sandy clay loam surface deposit with iron mottling and mixed modern and archaeological materials	-
			C.201	Dark reddish brown (5YR 2.5/2) to greyish brown (10YR 5/2) sandy clay loam containing mixed modern and archaeological (pottery and faunal bone) materials	-
	Phase II	2720-2490	C.202	Greyish brown (7.5YR 5/2) to brown (7.5YR 4/2) deposit with variable texture (sandy clay loam to loamy sand) containing pottery, clay pellets, faunal bones and bone artefacts.	H2_6
			F2-7	Very pale brown (10YR 7/3) compacted surface, c. 10 cm thick, containing pottery, faunal bones and charcoal. Falls within C.202 and covers most of the trench.	H2_6
		2760-2550	F2-13	Very dark brown (10YR 2/2) discrete area of charcoal, pottery, and faunal bones.	H2_5
			C.203	Very dark grey (7.5YR 3/10) sandy loam deposit containing pottery, charcoal and faunal bones, admixed with reworked fragments of compacted surfaces	-
	Phase I		C.204	Dark brown (7.5 YR 3/2) loamy sand layer c. 30 cm thick containing pottery, charcoal, faunal bones, bone artefacts and stone artefacts.	H2_4, H2_5
		3070-2790	F2-42	Reddish grey (5YR 5/2) compacted surface containing pottery and faunal bones. Several postholes were dug into the surface, showing a regular distribution in a NE-SW line.	H2_3
		3160-2970	F2-53	Greyish brown (2.5Y3/2) relatively hard compacted surface within C.204 located at the SW corner. It contains charcoal, pottery and animal bones, and postholes are dug into this feature.	H2_2
		3320-2960	C.205	Dark brown (7.5YR 3/2) to dark grey (5YR 4/1) sandy loam containing pottery, clay pellets, faunal bones, stone artefacts and charcoal.	H2_1, H2_2
	Sterile		C.206	Light brownish grey (2.5YR 6/2) natural (culturally sterile) loose sand deposit.	-

H1 = Trench 1. H2 = Trench 2. C. = Context. F = Feature

^Conventional radiocarbon ages have been calibrated in OxCal 4.4 (Bronk Ramsey 2009a) against a 50:50 mixture of the IntCal20 (Reimer et al. 2020) and SHCal20 (Hogg et al. 2020) calibration curves and quoted at 95.4% probability, rounded to ten years

Table 2 Calibrated and modelled ages (BP) within the 95% probability ranges for all the trenches excavated in 2012 and 2014 at Lo Gach using the General T-type Model (Model A) and the Charcoal Plus Outlier Model (Model B). The dates are listed in stratigraphic order within each trench with the oldest context at the bottom. Model B is shown in Fig. 3 and Model A is shown in Fig. S2.1

Trench	Name: Lab code	Conventional Radiocarbon Age (^{14}C age BP)	Unmodelled calibrated Dates		Model A: Modelled age (cal. BP)			Model B: Modelled age (cal. BP)		
			from	to	from	to		from	to	
			95% probability range		95% probability range		C	95% probability range		C
2012 Trial Trench	Boundary End Layer 3				2717	2477	100	2622	2446	97.9
	SANU-32637	2560±35	2751	2493	2717	2508	100	2622	2469	98.7
	Boundary =Start c.306				2718	2522	100	2623	2484	99
	Boundary End Layer 7				2721	2532	100	2626	2500	99.1
	S-ANU32638	2565±35	2752	2494	2722	2537	100	2628	2509	99.1
	Boundary Transition Layer 9/ Layer 7				2723	2540	100	2631	2515	99
	S-ANU32639	2455±35	2702	2354	2724	2542	100	2634	2519	98.9
	Boundary =Transition c.105/F1-123				2731	2544	100	2715	2524	98.5
	R_Combine LG004	2585±40; 2585±55	2756	2499	2744	2544	100	2739	2525	98.5
	Boundary Start Layer 12				2783	2543	100	2751	2525	98.4
Trench 1	Boundary End F1-8				2719	2529	100	2626	2489	99.1
	S-ANU38832	2510±25	2723	2466	2719	2532	100	2626	2493	99.2
	Boundary Transition F1-7/F1-8				2719	2535	100	2626	2496	99.2
	S-ANU38833	2560±25	2744	2498	2719	2538	100	2627	2499	99.2
	Boundary Transition F1-9/F1-7				2720	2538	100	2627	2502	99.2
	S-ANU43929	2513±25	2723	2469	2720	2539	100	2627	2505	99.2
	Boundary Transition F1-10/F1-9				2720	2539	100	2628	2508	99.2
	S-ANU43930	2568±25	2748	2500	2720	2541	100	2628	2510	99.2
	Boundary Transition F1-12/F1-10				2720	2541	100	2628	2513	99.2
	R_Combine SA-27 14LGa H1 F1-12 D2	2521±25; 2528±25	2724	2494	2721	2541	100	2629	2515	99.1
	Boundary Transition F1-15/F1-12				2721	2541	100	2629	2516	99.1
	S-ANU43928	2519±25	2725	2490	2722	2541	100	2629	2518	99
	Boundary Transition F1-110/F1-15				2722	2541	100	2630	2518	99
	S-ANU38829	2490±35	2718	2368	2722	2541	100	2630	2519	98.9
	Boundary Transition F1-121/F1-110				2723	2542	100	2631	2520	98.9

	S-ANU40636 (rice grain)	2530±20	2726	2494	2723	2544	100	2707	2523	98.8
	Boundary Transition F1-123/F1-121				2724	2544	100	2708	2524	98.8
	S-ANU38830	2535±25	2735	2493	2726	2544	100	2711	2524	98.7
	S-ANU40635 (rice grain)	2570±20	2747	2518	2727	2544	100	2710	2524	98.7
	Boundary Transition c.105/F1-123				2731	2544	100	2715	2524	98.5
	R_Combine SA-276	2655±30; 2790±45	2848	2750	2848	2750	100	2848	2750	100
	Boundary Start 105				2753	2543	100	2651	2523	98.1
Trench 2 (Phase II)	Boundary End 202_4				2729	2366	100	2720	2362	99.9
	S-ANU38913	2525±20	2724	2493	2727	2500	100	2722	2482	100
	Boundary Transition F2-3/202_4				2799	2541	100	2753	2527	100
	S-ANU38835	2705±30	2850	2752	2846	2619	100	2774	2597	100
	Boundary Transition F2-13/F2-3				2895	2643	100	2797	2622	100
	S-ANU38836	2605±25	2758	2547	2916	2717	100	2817	2662	100
	Boundary Start F2-13				2970	2727	100	2921	2686	100
Trench 2 (Phase I)	Boundary End F2-42				3056	2814	100	3020	2762	100
	S-ANU38837	2850±45	3074	2788	3067	2889	100	3045	2838	100
	S-ANU38914	2930±25	3154	2963	3076	2952	100	3055	2854	100
	Boundary Transition F2-53/F2-42				3112	2963	100	3093	2885	100
	S-ANU40634	2935±20	3157	2966	3142	2996	100	3123	2926	100
	Boundary Transition C205/F2-53				3182	3000	100	3166	2940	100
	S-ANU38838	2975±45	3318	2964	3216	3012	100	3205	2962	100
	Boundary Start C205				3355	3010	100	3323	2957	99.8
Trench 3	Boundary End Trench 3				2714	2475	100	2612	2406	98.5
	S-ANU38839	2570±25	2750	2500	2713	2494	100	2612	2417	99
	Boundary Transition F3-9/F3-5				2714	2497	100	2612	2426	99.1
	S-ANU38906	2465±20	2699	2361	2714	2500	100	2613	2435	99.2
	Boundary Transition c.303/F3-9				2714	2503	100	2614	2443	99.2
	S-ANU38907	2575±30	2753	2499	2714	2510	100	2615	2451	99.2
	Boundary Transition c.304/c.303				2715	2512	100	2616	2458	99.3
	S-ANU38909	2545±20	2737	2497	2714	2517	100	2617	2465	99.3
	Boundary Transition c.305/c.304				2716	2517	100	2618	2470	99.3

	S-ANU38911	2535±20	2729	2495	2717	2518	100	2619	2475	99.3
	S-ANU38910	2385±25	2486	2338	2717	2518	100	2619	2473	99.2
	Boundary Transition c.306/c.305				2717	2520	100	2621	2477	99.3
	S-ANU38912	2545±25	2740	2495	2717	2521	100	2622	2481	99.2
	Boundary Start c.306				2718	2522	100	2623	2484	99
	Boundary =End F1-8				2719	2529	100	2626	2489	99.1

Table 3 The modelled start and end dates for the phases of activity recorded in the 2012 Trial Trench and Trenches 1-3 using the General t-Type Outlier Model (Model A) and Charcoal Plus Outlier Model (Model B)

	MODEL A			**MODEL B**		
Trench	**Start Date (cal. BP)**	**End Date (cal. BP)**	**Interval (years)**	**Start Date (cal. BP)**	**End Date (cal. BP)**	**Interval (years)**
Trial Trench	2761-2545	2718-2526	0-197	2716-2528	2622-2492	0-121
1	2779-2544	2717-2479	0-222.5	2737-2527	2621-2448	0-179
2	3354-3010	2731-2369	321-875.5	3290-2942	2721-2402	277-786.5
3	2718-2528	2708-2464	0-204.5	2623-2494	2552-2400	0-149.5

Table 4 Lo Gach microfacies types: summary of microarchaeological (micromorphological and compositional) attributes and depositional history. Microarchaeological data according to sample number (full micromorphological descriptions, representative FTIR spectra and phytolith concentrations) are provided in Supplementary Material 4

Representative photomicrograph	mF	Micromorphology summary	FTIR mineral compositions	Biogenic silica concentrations (per 1g sediment)	Depositional history
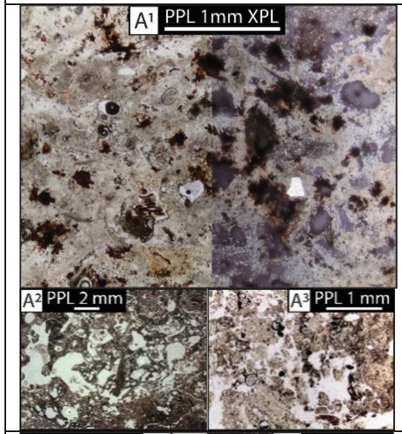	A	• mF A^1: Massive deposit of weathered and recrystallised calcitic plant ashes that are post-depositionally impregnated with Fe-Mn oxide dendrites. • mF A^2: Vitrified phytolith slags, conferring a vesicular structure to the deposit. • mF A^3: A post-depositional variant, comprising a biological granular structure of excremental aggregates and finely comminuted combusted and ashed plant residues	• mF A^1: Cl(a.) > Opal > Arg = Cal > Qtz > CHAP. • mF A^2: Glass (vitrified phytoliths) > Opal > Cal > CHAP. • mF A^3: Cl(a.) > Opal > Cal > Gp > CHAP.	• mF A^1: Phytoliths: 194,000-2,411,000. Diatoms: 0-3,335,000. • mF A^2: Phytoliths: 136,000. No diatoms. • mF A^3: Phytoliths: 0-613,000. No diatoms.	Ashed plant residues with massive, unsorted fabric arrangements and lack of evidence for *in situ* burning, indicating remobilisation from the place of burning and redeposition in a secondary midden context: • mF A^1: Calcitic ashes from the burning of woody plants. The calcitic ashes form compacted, recrystallised masses from wet burial conditions and possibly trampling. Subsequent dry conditions are indicated by bioturbation, desiccation cracks, phosphatisation, and widespread precipitation of authigenic gypsum, secondary calcite, and iron and manganese. • mF A^2: Vitrified phytolith slags from the high temperature (>800°C) burning of phytolith-rich plants (e.g., grasses and/or reeds) • mF A^3: Combustion residues that underwent intensive bioturbation, resulting in transformation of microstructures and components into homogenised microaggregates and crumbs.
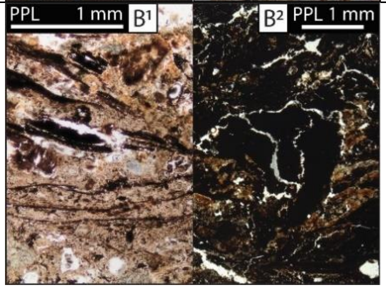	B	• mF B^1: Massive deposits of carbonised plant remains, often organised in horizontally-oriented, parallel arrangements and associated with a phosphatised ashy micromass • mF B^2: Large fragments of horizontally-oriented wood charcoal, comprising a laterally continuous microlayer	• mF B^1: Cl(a.) > Gp > Opal > Cl(n.a.) > Qtz > CHAP. • mF B^2: Charcoal > Cl(a.) > Qtz.	• mF B^1: Phytoliths: 147,000. Diatoms: 206,000. • mF B^2: Phytoliths: 279,000. No diatoms.	• mF B^1: Carbonised plant residues from the burning of woody plants. The lack of evidence for *in situ* burning suggests the residues have been mobilised to a secondary location such as a midden. The finely laminated, compacted microstructures indicate that the deposit experienced surface trampling. • mF B^2: Continuous microlayer of large, horizontally-oriented fragments of charcoal representing the discard of combustion residues or possibly an *in situ* conflagration event.
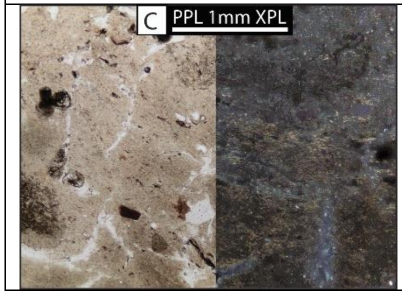	C	mF C: Massive, homogenous deposit of well-oriented, non-burnt silty clays. The clays are relatively pure and contain horizontally-oriented diatoms and infrequent charcoal and bone fragments. Voids include vesicles and planar cracks.	Cl(n.a.) > Qtz > CHAP > Opal*.	Phytoliths: 491,000-1,016,000. Diatoms: 982,000-4,106,000.	Clay plastered floor surface. The clays were sourced from local diatom-rich alluvial or swampy environments (indicated by high concentrations of diatoms) and were worked into a wet, plastic-like consistency (indicated by well-oriented clay domains and horizontal orientation of inclusions). Disaggregation of fabric and formation of planar voids along the upper surface could have resulted from trampling or sweeping.

Numerical superscripts following mF types denote sub-groupings of particular microfacies based on slight variations in composition

FTIR mineralogical identifications: Arg = Aragonite. Cal = Calcite. CHAP = Carbonated hydroxyapatite. Gp = Gypsum. Qtz = Quartz. Clay alteration state: Cl(n.a.) = clay not altered (not heated). Cl(s.a.) = clay slightly altered (possibly altered (heated) clay, however mixture of altered and non-altered clay or other materials masks the signal of strong heat-induced clay alteration). Cl(a) = altered (heated). * = Possible presence of opal as a minor constituent

Table 4 (cont.) Summary of Lo Gach microfacies types

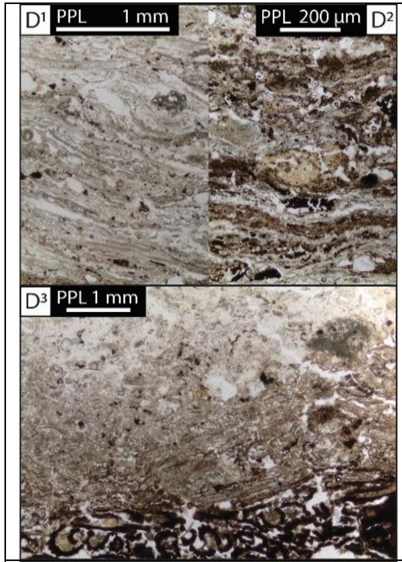	D	• mF D^1: articulated phytoliths and silicified plant fibres, mostly rice husks, in anatomical connection and arranged in a laminated microstructure. • mF D^2: variant of mF D^1 sharing a similar laminated structure and dominance of articulated phytoliths, with addition of horizontally-oriented, crushed bone and charcoal fragments and lenses of amorphous organic matter compressed between the phytolith laminations. • mF D^3: variant of mF D^1, showing a microstratigraphic gradation in colour from pale grey (ashed) through to black (carbonised)	• mF D^1: Opal > Gp. • mF D^2: Gp > Opal > Cl(s.a.) = Cl(n.a.) > Cal > Qtz > CHAP.	• mF D^2: Phytoliths: 2,257,000. No diatoms.	Decay of plant remains *in situ*, producing horizontally-oriented phytoliths and silicified plant fibres in anatomical connection. Deposits subsequently experienced intensive trampling, producing a finely laminated, compacted and undulating microstructure. • mF D^1: Plant remains derive predominantly from rice plants, indicating the discard of rice processing waste. • mF D^2: In addition to dominant silicified plant fibres and rice husks, deposits contain heterogenous inclusions occurring as 'stringers' and horizontally-oriented fragments crushed *in situ* and compressed between the phytoliths: bone, charcoal, shell, vitrified phytolith slags, amorphous organic matter, clay plaster fragments, pottery sherds, detrital quartz grains and sandstone clasts. This indicates a combination of waste from different activities. • mF D^3: Horizontally oriented, finely laminated rice husks showing *in situ* gradation of ashed (top) to carbonised (bottom), indicating *in situ* burning of plant processing waste. Reversed microstratigraphy observed in one sample (carbonised (top) to ashed (bottom)) may have resulted from hearth sweeping and rake-out activities.
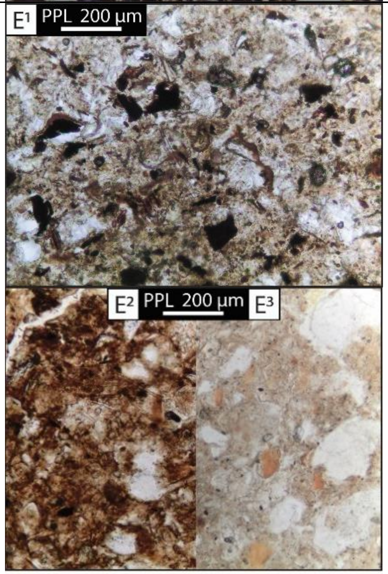	E	mF E: biological peds containing finely comminuted and well-homogenised anthropogenic inclusions. Three subtypes, mFs E^1, E^2 and E^3, are distinguished based on differences in groundmass composition: • mF E^1: pale grey (PPL) fine material containing concentrations of charcoal, phytoliths, and silicified plant remains including rice husks and vitrified silica slags. • mF E^2: dotted dark brown (PPL) amorphous fine organic matter with concentrations of embedded phytoliths and burnt and unburnt bone fragments. • mF E^3: pale cream (PPL) fine material containing concentrations of rice husks, phytoliths and small, rounded and weathered bone fragments.	• mF E^1: Gp = Cl(n.a.) > Qtz. • mF E^2: Cl(n.a.) = Cl(a.) = Cl(s.a.) > Qtz > OPAL > CHAP. • mF E^3: Cl(a.) > Qtz > Opal > CHAP.	• mF E^1: Phytoliths: 1,128,000. Diatoms: 629,000. • mF E^2: Phytoliths: 264,000-2,426,000. Diatoms: 176,000-2,029,000. • mF E^3: Phytoliths: 430,000. Diatoms: 523,000.	Dumping of waste materials in a secondary midden context. • mF E^1: waste related to burning activities due to concentrations of charcoal, burnt bone and vitrified phytolith slags. • mF E^2: waste related to animal processing activities due to the dominance of bone fragments. • mF E^3: waste related to plant processing and food preparation activities, due to the dominance of rice husks and unburnt bone. Phosphatic features in mF E^3 possibly derive from human or animal faecal waste. Trampling took place on exposed surfaces during pauses in midden deposition. The cultural components have been comminuted and transformed into soil peds through the actions of soil biota.

REFERENCES

Albert RM, Shahack-Gross R, Cabanes D, Gilboa A, Lev-Yadun S, Portillo M, Sharon I, Boaretto E, Weiner S (2008) Phytolith-rich layers from the Late Bronze and Iron Ages at Tel Dor (Israel): mode of formation and archaeological significance. J Archaeol Sci 35:57–75

Aldeias V, Goldberg P, Sandgathe D, Berna F, Dibble HL, McPherron SP, Turq A, Rezek Z (2012) Evidence for Neandertal use of fire at Roc de Marsal (France). J Archaeol Sci 39:2414–2423

Balbo AL, Cabanes D, Garcia-Granero JJ, Bonet A, Ajithprasad P, Terradas X, (2015) A microarchaeological approach for the study of pits. Environ Archaeol 20:390–405

Banerjea RY, Bell M, Matthews W, Brown A (2015a) Applications of micromorphology to understanding activity areas and site formation processes in experimental hut floors. Archaeol Anthropol Sci 7:89–112

Banerjea RY, Fulford M, Bell M, Clarke A, Matthews W (2015b) Using experimental archaeology and micromorphology to reconstruct timber-framed buildings from Roman Silchester: a new approach. Antiquity 89:1174–1188

Barton H, Denham T (2011) Prehistoric vegeculture and social life in Island Southeast Asia and Melanesia. In: Barker G, Janowski M (eds) Why Cultivate? Anthropological and archaeological approaches to foraging-farming transitions in Southeast Asia. McDonald Institute for Archaeological Research, University of Cambridge, Cambridge, pp 17–25

Bergada MM, Poch RM, Cervello JM (2015) On the presence of gypsum in the archaeological burial site of Cova des Pas (Menorca, western Mediterranean). J Archaeol Sci 53:472–481

Berna F, Matthews A, Weiner S (2004) Solubilities of bone mineral from archaeological sites: the recrystallization window. J Archaeol Sci 31:867–882

Bernot L (1982) The house of swidden farmers as a special object for ethnological study. In: Izikowitz KG, Sorensen P (eds) The House in East and Southeast Asia: anthropological and architectural aspects. Curzon Press, London, pp 35–40

Braadbaart F, Poole I (2008) Morphological, chemical and physical changes during charcoalification of wood and its relevance to archaeological contexts. J Archaeol Sci 35:2434–2445

Braadbaart F, Poole I, Huisman HD, van Os B (2012) Fuel, fire and heat: an experimental approach to highlight the potential of studying ash and char remains from archaeological contexts. J Archaeol Sci 39:836–847

Brochier JE, Thinon M (2003) Calcite crystals, starch grains aggregates or… POCC? Comment on 'calcite crystals inside archaeological plant tissues.' J Archaeol Sci 30:1211–1214

Bronk Ramsey C (2009a) Bayesian analysis of radiocarbon dates. Radiocarbon 51:337–360

Bronk Ramsey C (2009b) Dealing with outliers and offsets in radiocarbon dating. Radiocarbon 51:1023–1045

Bui PD, Reinecke A, Nguyen MX, Van BN (2003) Report on the Second Excavation at Go O Chua (May 2003). Long An Provincial Museum, Vietnam National Museum of History, Hanoi

Bui VL (2008) Di chi Lo Gach [Lo Gach site] (Long An Province). Khao Co Hoc 2:26–44

Cameron J (2017) Matting impressions from Lo Gach: materiality at floor level. In: Piper PJ, Matsumara H, Bulbeck D (eds) New Perspectives in Southeast Asian and Pacific Prehistory. ANU Press, Canberra, pp 357–367

Canti M (2003) Aspects of the chemical and microscopic characteristics of plant ashes found in archaeological soils. Catena 54:339–361

Canti M (2017) Charred Plant Remains. In: Nicosia C, Stoops G (eds) Archaeological Soil and Sediment Micromorphology. John Wiley and Sons, Hoboken, NJ, pp 141–142

Canti M, Brochier JE (2017) Plant ash. In: Nicosia C, Stoops G (eds) Archaeological Soil and Sediment Micromorphology. John Wiley and Sons, Hoboken, NJ, pp 147–154

Cobo-Castillo C (2018) Preservation bias: is rice overrepresented in the archaeological record? Archaeol Anthropol Sci https://doi.org/10.1007/s12520-018-0717-4

Cohen DJ (2011) The beginnings of agriculture in China. Curr Anthropol 52:S273–S293

Courty M-A (2001) Microfacies analysis assisting archaeological stratigraphy. In: Goldberg P, Holliday V, Ferring C (eds) Earth Sciences and Archaeology. Kluwer Academic/Plenum Publishers, New York, pp 205–239

Courty M-A, Goldberg P, Macphail RI (1989) Soils and Micromorphology in Archaeology. Cambridge University Press, Cambridge

Courty M-A, Goldberg P, Macphail RI (1994) Ancient people: lifestyles and cultural patterns. In: Wilding L (ed) Proceedings of the International Soil Science Society. International Soil Science Society, Acapulco, pp 250–269

Duke BJ, Carter AK, Chang NJ (2011) The excavation of Iron Age working floors and small-scale industry at Ban Non Wat, Thailand. Papers from the Institute of Archaeology 20:123–130

Flad RK, Yuan J, Li S (2007) Zooarcheological evidence for animal domestication in northwest China. In: Madsen DB, Chen FH, Gao X (eds) Late Quaternary Climate Change and Human Adaptation in Arid China 9:167–204

Friesem DE, Tsartsidou G, Karkanas P, Shahack-Gross R (2014) Where are the roofs? A geo-ethnoarchaeological study of mud brick structures and their collapse processes, focusing on the identification of roofs. Archaeol Anthropol Sci 6:73–92

Friesem DE, Lavi N, Madella M, Ajithprasad P, French C (2016) Site formation processes and hunter-gatherers use of space in a tropical environment: a geo-ethnoarchaeological approach from South India. PloS one 11:1–30

Friesem DE, Lavi N (2017) Foragers, tropical forests and the formation of archaeological evidences: an ethnoarchaeological view from South India. Quat Int 448:117–128

Ge T, Courty M-A, Mattews W, Wattez J (1993) Sedimentary formation processes of occupation surfaces. In: Goldberg P, Nash D, Petraglia M (eds) Formation Processes in Archaeological Context. Prehistory Press, Madison, Wisconsin, pp 149–163

Goldberg P, Berna F (2010) Micromorphology and context. Quat Int 214:56–62

Goldberg P, Miller CE, Schiegl S, Ligouis B, Berna F, Conard NJ, Wadley L (2009) Bedding, hearths, and site maintenance in the Middle Stone age of Sibudu cave, KwaZulu-Natal, South Africa. Archaeol Anthropol Sci 1:95–122

Goldberg P, Whitbread I (1993) Micromorphological study of a Bedouin tent floor. In: Goldberg P, Nash D, Petraglia M (eds) Formation Processes in Archaeological Context. Prehistory Press, Madison, Wisconsin, pp 165–188

Graham E, Macphail RI, Turner S, Crowther J, Stegemann J, Arroyo-Kalin M, Duncan L, Whittet R, Rosique C, Austin P (2015) The Marco Gonzalez Maya site, Ambergris Caye, Belize: assessing the impact of human activities by examining diachronic processes at the local scale. Quat Int 437:115–142

Grave P, Kealhofer L (1999) Assessing bioturbation in archaeological sediments using soil morphology and phytolith analysis. J Archaeol Sci 26:1239–1248

Grono E (2020) Settlement at the Micro-scale: Microstratigraphy and micromorphology of transitional Neolithic settlement sites in Vietnam (5000 cal BP to 2500 cal BP). PhD Thesis, Australian National University, Canberra

Grono E, Piper PJ, Dang KN, Bellwood P, Denham T, Friesem DE (in press) Early settlement construction in Southeast Asia: lime mortar floor sequences at Loc Giang, southern Vietnam. Antiquity

Grono E, Piper PJ, Nguyen KTK, Dang KN, Denham T, Friesem DE (2022) The identification of dwellings and site formation processes at archaeological settlements in the tropics: a micro-geoarchaeological case study from neolithic Loc Giang, southern Vietnam. Quat Sci Rev 291:107654

Hardy-Smith T, Edwards PC (2004) The garbage crisis in prehistory: artefact discard patterns at the Early Natufian site of Wadi Hammeh 27 and the origins of household refuse disposal strategies. J Anthropol Archaeol 23:253–289

Henriksen MA (1982) The first excavated prehistoric house site in Southeast Asia. In: Izikowitz KG, Sorensen P (eds) The House in East and Southeast Asia: anthropological and architectural aspects. Curzon Press, London, pp 17–24

Higham CFW (2014) Early Mainland Southeast Asia: from first humans to Angkor. River Books, Bangkok

Higham CFW (2017) The prehistoric house: a missing factor in Southeast Asian history. In: Piper PJ, Matsumara H, Bulbeck D (eds) New Perspectives in Southeast Asian and Pacific Prehistory. ANU Press, Canberra, pp 369–384

Higham CFW, Kijngam A (2012) The Origins of The Civilization of Angkor. Volume 6: the excavation of Ban Non Wat. The Iron Age, summary and conclusions. The Fine Arts Department of Thailand, Bangkok

Higham CFW, Cameron J, Chang N, Castillo C, Halcrow S, O'Reilly D, Petchey F, Shewan L (2014) The excavation of Non Ban Jak, Northeast Thailand: a report on the first three seasons. J Indo-Pacific Archaeol 34:1–41

Higham CFW, Cawte H (2021) Bronze Metallurgy in Southeast Asia with Particular Reference to Northeast Thailand. J World Prehist 1–46

Hogg AG, Heaton TJ, Hua Q, Palmer JG, Turney CS, Southon J, Bayliss A, Blackwell PG, Boswijk G, Bronk Ramsey C (2020) SHCal20 Southern Hemisphere calibration, 0–55,000 years cal BP. Radiocarbon 62:759–778

Hori H (2000) The Mekong: environment and development. United Nations University Press, Tokyo

Huisman DJ, Jongmans AG, Raemaekers DCM (2009) Investigating Neolithic land use in Swifterbant (NL) using micromorphological techniques. Catena 78:185–197

Huisman DJ, Braadbaart F, van Wijk IM, van Os BJH (2012) Ashes to ashes, charcoal to dust: micromorphological evidence for ash-induced disintegration of charcoal in Early Neolithic (LBK) soil features in Elsloo (The Netherlands). J Archaeol Sci 39:994–1004

Huisman DJ, Raemaekers DCM (2014) Systematic cultivation of the Swifterbant wetlands (The Netherlands). Evidence from Neolithic tillage marks (c. 4300–4000 cal. BC). J Archaeol Sci 49:572–584

Hutson SR, Stanton TW, Magnoni A, Terry R, Craner J (2007) Beyond the buildings: formation processes of ancient Maya houselots and methods for the study of non-architectural space. J Anthropol Archaeol 26:442–473

Kadowaki S, Maher L, Portillo M, Albert RM, Akashi C, Guliyev F, Nishiaki Y (2015) Geoarchaeological and palaeobotanical evidence for prehistoric cereal storage in the southern Caucasus: the Neolithic settlement of Goytepe (mid 8th millennium BP). J Archaeol Sci 53:408–425

Kanthilatha N, Boyd W, Dowell A, Mann A, Chang N, Wohlmuth H, Parr J, (2014) Identification of preserved fatty acids in archaeological floor sediments from prehistoric sites at Ban Non Wat and Nong Hua Raet in northeast Thailand using gas chromatography. J Archaeol Sci 46:353–362

Karkanas P (2017) Chemical alteration. In: Gilbert AS, Goldberg P, Holliday VT, Mandel RD, Sternberg RS (eds) Encyclopedia of Geoarchaeology. Springer, Dordrecht, pp 129–138

Karkanas P, Bar-Yosef O, Goldberg P, Weiner S (2000) Diagenesis in prehistoric caves: the use of minerals that form in situ to assess the completeness of the archaeological record. J Archaeol Sci 27:915–929

Karkanas P, Goldberg P (2010) Phosphatic features. In: Stoops G, Marcelino V, Mees F (eds) Interpretation of Micromorphological Features of Soils and Regoliths. Elsevier, Amsterdam, pp 521–541

Karkanas P, Goldberg P (2018) Reconstructing Archaeological Sites: understanding the geoarchaeological matrix. John Wiley & Sons, Hoboken, NJ

Karkanas P, Shahack-Gross R, Ayalon A, Bar-Matthews M, Barkai R, Frumkin A, Gopher A, Stiner MC (2007) Evidence for habitual use of fire at the end of the Lower Paleolithic: site-formation processes at Qesem Cave, Israel. J Hum Evol 53:197–212

Karkanas P, Van de Moortel A (2014) Micromorphological analysis of sediments at the Bronze Age site of Mitrou, central Greece: patterns of floor construction and maintenance. J Archaeol Sci 43:198–213

Katz O, Cabanes D, Weiner S, Maeir AM, Boaretto E, Shahack-Gross R (2010) Rapid phytolith extraction for analysis of phytolith concentrations and assemblages during an excavation: an application at Tell es-Safi/Gath, Israel. J Archaeol Sci 37:1557–1563

Kourampas N, Simpson IA, Perera N, Deraniyagala SU, Wijeyapala WH (2009) Rockshelter sedimentation in a dynamic tropical landscape: late Pleistocene–early Holocene archaeological deposits in Kitulgala Beli-lena, southwestern Sri Lanka. Geoarchaeology 24:677–714

Lewis H (2007) Preliminary soil micromorphology studies of landscape and occupation history at Tabon Cave, Palawan, Philippines. Geoarchaeology 22, 685–708

Lindbo DL, Stolt MH, Vepraskas MJ (2010) Redoximorphic features. In: Stoops G, Marcelino V, Mees F (eds) Interpretation of Micromorphological Features of Soils and Regoliths. Elsevier, Amsterdam, pp 129–147

Macphail RI (2017) Privies and latrines. In: Gilbert AS, Goldberg P, Holliday VT, Mandel RD, Sternberg RS (eds) Encyclopedia of Geoarchaeology. Springer, Dordrecht, pp 682–687

Macphail RI, Goldberg P (2010) Archaeological materials. In: Stoops G, Marcelino V, Mees F (eds) Interpretation of Micromorphological Features of Soils and Regoliths. Elsevier, Amsterdam, pp 589–622

Macphail RI, Goldberg P (2017) Applied Soils and Micromorphology in Archaeology. Cambridge University Press, Cambridge

Mallol C, Hernandez CM, Cabanes D, Machado J, Sistiaga A, Perez L, Galvan B (2013) Human actions performed on simple combustion structures: an experimental approach to the study of Middle Palaeolithic fire. Quat Int 315:3–15

Mallol C, Mentzer SM, Miller CE (2017) Combustion features. In: Nicosia C, Stoops G (eds) Archaeological Soil and Sediment Micromorphology. John Wiley and Sons, Hoboken, NJ, pp 299–330

Matthews W (2005) Micromorphological and microstratigraphic traces of uses and concepts of space. In: Hodder I (ed) Inhabiting Catalhoyuk: reports from the 1995–1999 seasons. McDonald Institute for Archaeological Research and British Institute of Archaeology at Ankara, Cambridge, pp 355–98

Matthews W, French CA, Lawrence T, Cutler DF, Jones MK (1997) Microstratigraphic traces of site formation processes and human activities. World Archaeol 29:281–308

Matthews W, Postgate JN (1994) The imprint of living in an early Mesopotamian city: questions and answers. In: Ruff L, Rowley-Conway P (eds) Whither Environmental Archaeology? Oxbow, Oxford, pp 171–212

McAdams C, Morley MW, Fu X, Kandyba AV, Derevianko AP, Nguyen DT, Doi NG, Roberts RG (2019) The Pleistocene geoarchaeology and geochronology of Con Moong Cave, North Vietnam: site formation processes and hominin activity in the humid tropics. Geoarchaeology https://doi.org/10.1002/gea.21758:

Mentzer SM (2014) Microarchaeological approaches to the identification and interpretation of combustion features in prehistoric archaeological sites. J Archaeol Method Theory 21:616–668

Milek KB (2012) Floor formation processes and the interpretation of site activity areas: an ethnoarchaeological study of turf buildings at Thvera, northeast Iceland. J Anthropol Archaeol 31:119–137

Miller CE, Conard NJ, Goldberg P, Berna F (2010) Dumping, sweeping and trampling: experimental micromorphological analysis of anthropogenically modified combustion features. Palethnologie 2:25–37

Miller CE, Sievers C (2012) An experimental micromorphological investigation of bedding construction in the Middle Stone Age of Sibudu, South Africa. J Archaeol Sci 39:3039–3051

Morley MW, Goldberg P (2017) Geoarchaeological research in the humid tropics: a global perspective. J Archaeol Sci 77:1–9

Morley MW, Goldberg P, Sutikna T, et al (2017) Initial micromorphological results from Liang Bua, Flores (Indonesia): site formation processes and hominin activities at the type locality of Homo floresiensis. J Archaeol Sci 77:125–142

Nguyen VL, Ta TKO, Tateishi M (2000) Late Holocene depositional environments and coastal evolution of the Mekong River Delta, southern Vietnam. J Asian Earth Sci 18:427–439

Nicosia C, Stoops G (2017) Archaeological Soil and Sediment Micromorphology. John Wiley and Sons, Hoboken, NJ

Nishimura M, Nguyen KD (2002) Excavation of An Son: a Neolithic mound site in the middle Vam Co Dong valley, southern Vietnam. Bulletin of the Indo-Pacific Prehistory Association 22:101–109. https://doi.org/10.7152/bippa.v22i0.11810

Nitta E (1991) Archaeological study on the ancient iron-smelting and salt-making industries in the northeast of Thailand. Preliminary report on the excavations of Non Yang and Ban Don Phlong. J Southeast Asian Archaeol 11:1–46

O’Reilly DJ (1997) The discovery of clay-lined floors at an Iron Age site in Thailand: preliminary observations from Non Muang Kao, Nakon Ratchasima Province. J Siam Soc 85:1–14

O’Reilly DJ (2014) Increasing complexity and the political economy model: a consideration of Iron Age moated sites in Thailand. J Anthropol Archaeol 35:297–309

Oxenham MF, Piper PJ, Bellwood P, Bui CH, Nguyen KTK, Nguyen QM, Campos F, Castillo C, Wood R, Sarjeant C, Amano N, Willis A, Ceron J, (2015) Emergence and diversification of the Neolithic in Southern Vietnam: insights from coastal Rach Nui. J Island Coast Archaeol 10(3):309–339

Piper PJ, Oxenham MF (2014) Of prehistoric pioneers: the establishment of the first sedentary settlements in the Mekong Delta Region of southern Vietnam during the Period 2000-1500 cal. BC. In: Boyle K, Rabett R, Hunt CO (eds) Living in the Landscape: essays in honour of Graeme Barker. McDonald Institute for Archaeological Research, Cambridge, pp 209–226

Piper PJ, Nguyen KTK, Tran TKQ, Wood R, Cobo-Castillo C, Weisskopf A, Campos F, Dang NK, Sarjeant C, Mijares AS, Oxenham MF, Bellwood P (2017) The Neolithic settlement of Loc Giang on the Vam Co Dong River, southern Vietnam and its broader regional context. Archaeol Res Asia 10:32–47

Proske U, Hanebuth TJ, Behling H, et al (2010) The palaeoenvironmental development of the northeastern Vietnamese Mekong River Delta since the mid Holocene. Holocene 20:1257–1268

Proske U, Heslop D, Hanebuth TJ (2009) Salt production in pre-Funan Vietnam: archaeomagnetic reorientation of briquetage fragments. J Archaeol Sci 36:84–89

Rathje WL, Murphy C (1992) Rubbish!: the archaeology of garbage. HarperCollins, New York

Regev L, Cabanes D, Homsher R, Kleiman A, Weiner S, Finkelstein I, Shahack-Gross R (2015) Geoarchaeological investigation in a domestic iron age quarter, Tel Megiddo, Israel. Bulletin of the American Schools of Oriental Research 374:135–157

Reimer PJ, Austin WE, Bard E, Bayliss A, Blackwell PG, Bronk Ramsey C, Butzin M, Cheng H, Edwards RL, Friedrich M (2020) The IntCal20 Northern Hemisphere radiocarbon age calibration curve (0–55 cal kBP). Radiocarbon 62:725–757

Rentzel P, Narten G-B (2000) Zur Entstehung von Gehniveaus in sandig-lehmigen Ablagerungen: Experimente und archaologische Befunde. Jahresbericht der Archäologischen Bodenforschung des Kantons Basel-Stadt 1999:107–127

Rentzel P, Nicosia C, Gebhardt A, Bronnimann D, Pumpin C, Ismail-Meyer K (2017) Trampling, poaching and the effect of traffic. In: Nicosia C, Stoops G (eds) Archaeological Soil and Sediment Micromorphology. John Wiley and Sons, Hoboken, NJ, pp 281–297

Robin C (2002) Outside of houses: the practices of everyday life at Chan Noohol, Belize. J Soc Archaeol 2:245–268

Robin C, Rothschild NA (2002) Archaeological ethnographies: Social dynamics of outdoor space. J Soc Archaeol 2:159–172

Schiegl S, Goldberg P, Pfretzschner H-U, Conard NJ (2003) Paleolithic burnt bone horizons from the Swabian Jura: distinguishing between in situ fireplaces and dumping areas. Geoarchaeology 18:541–565

Shahack-Gross R (2011) Herbivorous livestock dung: formation, taphonomy, methods for identification, and archaeological significance. J Archaeol Sci 38:205–218

Shahack-Gross R (2017) Animal gathering enclosures. In: Nicosia C, Stoops G (eds) Archaeological Soil and Sediment Micromorphology. John Wiley and Sons, Hoboken, NJ, pp 265–280

Shahack-Gross R, Berna F, Karkanas P, Weiner S (2004) Bat guano and preservation of archaeological remains in cave sites. J Archaeol Sci 31:1259–1272

Shahack-Gross R, Albert R-M, Gilboa A, Nagar-Hilman O, Sharon I, Weiner S, (2005) Geoarchaeology in an urban context: the uses of space in a Phoenician monumental building at Tel Dor (Israel). J Archaeol Sci 32:1417–1431

Shahack-Gross R, Gafri M, Finkelstein I (2009) Identifying threshing floors in the archaeological record: a test case at Iron Age Tel Megiddo, Israel. J Field Archaeol 34:171–184

Shillito L-M, Bull ID, Matthews W, Almond MJ, Williams JM, Evershed RP (2011a) Biomolecular and micromorphological analysis of suspected faecal deposits at Neolithic Catalhoyuk, Turkey. J Archaeol Sci 38:1869–1877

Shillito L-M, Matthews W (2013) Geoarchaeological investigations of midden-formation processes in the Early to Late Ceramic Neolithic levels at Catalhoyuk, Turkey ca. 8550–8370 cal BP. Geoarchaeology 28:25–49

Shillito L-M, Matthews W, Almond MJ, Bull ID (2011b) The microstratigraphy of middens: capturing daily routine in rubbish at Neolithic Catalhoyuk, Turkey. Antiquity 85:1024–1038

Shillito L-M, Ryan P (2013) Surfaces and streets: phytoliths, micromorphology and changing use of space at Neolithic Catalhoyuk (Turkey). Antiquity 87:684–700

Simpson I, Kourampas N, Perera HN (2008) Bellan-bandi Palassa, Sri Lanka: formation processes of a Mesolithic open-air site identified through thin section micromorphology. Archaeologia: Journal of Archaeology 4:3–18

Sordoillet D, Weller O, Rouge N, Buatier M, Sizun J-P (2018) Earliest salt working in the world: From excavation to microscopy at the prehistoric sites of Ţolici and Lunca (Romania). J Archaeol Sci 89:46–55

Stattegger K, Tjallingii R, Saito Y, et al (2013) Mid to late Holocene sea-level reconstruction of Southeast Vietnam using beachrock and beach-ridge deposits. Glob Planet Change 110:214–222

Stephens M, Rose J, Gilbertson D, Canti M (2005) Micromorphology of cave sediments in the humid tropics: Niah Cave, Sarawak. Asian Perspectives 44:42–55

Stephens M, Rose J, Gilbertson DD (2017) Post-depositional alteration of humid tropical cave sediments: micromorphological research in the Great Cave of Niah, Sarawak, Borneo. J Archaeol Sci 77:109–124

Sulas F, Madella M (2012) Archaeology at the micro-scale: micromorphology and phytoliths at a Swahili stonetown. Archaeol Anthropol Sci 4:145–159

Sulas F, Fleisher J, Wynne-Jones S (2017) Geoarchaeology of urban space in tropical island environments: Songo Mnara, Tanzania. J Archaeol Sci 77:52–63

Ta TKO, Nguyen VL, Tateishi M, et al (2002) Sediment facies and Late Holocene progradation of the Mekong River Delta in Bentre Province, southern Vietnam: an example of evolution from a tide-dominated to a tide-and wave-dominated delta. Sediment Geol 152:313–325

Toffolo MB, Boaretto E (2014) Nucleation of aragonite upon carbonation of calcium oxide and calcium hydroxide at ambient temperatures and pressures: a new indicator of fire-related human activities. J Archaeol Sci 49:237–248

Tran TKQ, Piper PJ (2018) The transition from hunting to animal management in southern Vietnam. Paper presented at the 21st Congress of the Indo-Pacific Prehistory Association, 23-28 September, 2018, Hue, Vietnam

Villagran XS (2014) A redefinition of waste: deconstructing shell and fish mound formation among coastal groups of southern Brazil. J Anthropol Archaeol 36:211–227

Villagran XS, Balbo AL, Madella M, Vila A, Estevez J (2011) Stratigraphic and spatial variability in shell middens: microfacies identification at the ethnohistoric site Tunel VII (Tierra del Fuego, Argentina). Archaeol Anthropol Sci 3:357–378

Villagran XS, Huisman DJ, Mentzer SM, Miller CE, Jans MM (2017a) Bone and other skeletal tissues. In: Nicosia C, Stoops G (eds) Archaeological Soil and Sediment Micromorphology. John Wiley and Sons, Hoboken, NJ, pp 11–38

Villagran XS, Strauss A, Miller C, Ligouis B, Oliveira R (2017b) Buried in ashes: site formation processes at Lapa do Santo rockshelter, east-central Brazil. J Archaeol Sci 77:10–34

Wadley L, Sievers C, Bamford M, Goldberg P, Berna F, Miller C (2011) Middle Stone Age bedding construction and settlement patterns at Sibudu, South Africa. Science 334:1388–1391

Waterson R (1990) The Living House: an anthropology of architecture in south-East Asia. Oxford University Press, Singapore

Weiner S (2010) Microarchaeology: beyond the visible archaeological record. Cambridge University Press, Cambridge

White JC, Eyre CO (2011) Residential burial and the Metal Age of Thailand. In: Adams RL, King SM (eds) Residential Burial: a multiregional exploration. Archaeological Papers of the American Anthropological Association 20, Arlington, VA, 59–78